SANDIA REPORT

SAND2003-0706
Unlimited Release
Printed March 2003

Statistical Validation of Engineering and Scientific Models: Validation Experiments to Application

Richard G. Hills and Ian H. Leslie

Prepared by
Sandia National Laboratories
Albuquerque, New Mexico 87185 and Livermore, California 94550

Sandia is a multiprogram laboratory operated by Sandia Corporation, a Lockheed Martin Company, for the United States Department of Energy under Contract DE-AC04-94AL85000

Issued by Sandia National Laboratories, operated for the United States Department of Energy by Sandia Corporation.

Available to DOE and DOE contractors from
U.S. Department of Energy
Office of Scientific and Technical Information
P.O. Box 62
Oak Ridge, TN 37831

Telephone: (865)576-8401
Facsimile: (865)576-5782
E-Mail: reports@adonis.osti.gov
Online ordering: http://www.doe.gov/bridge

Available to the public from
U.S. Department of Commerce
National Technical Information Service
5285 Port Royal Rd
Springfield, VA 22161

Telephone: (800)553-6847
Facsimile: (703)605-6900
E-Mail: orders@ntis.fedworld.gov
Online order: http://www.ntis.gov/ordering.htm

SAND2003-0706
Unlimited Release
Printed March 2003

Statistical Validation of Engineering and Scientific Models: Validation Experiments to Application

Richard G. Hills and Ian H. Leslie
Department of Mechanical Engineering
New Mexico State University
Las Cruces, New Mexico 88003

Abstract

Several major issues associated with model validation are addressed here. First, we extend the application-based, model validation metric presented in Hills and Trucano (2001) to the Maximum Likelihood approach introduced in Hills and Trucano (2002). This method allows us to use the target application of the code to weigh the measurements made from a validation experiment so that those measurements that are most important for the application are more heavily weighted.

Secondly, we further develop the linkage between suites of validation experiments and the target application so that we can 1) provide some measure of coverage of the target application and, 2) evaluate the effect of uncertainty in the measurements and model parameters on application level validation. We provide several examples of this approach based on steady and transient heat conduction, and shock physics applications.

(Page left blank)

Acknowledgements

This report is an account of contract research (Doc. # AX-0620) performed by the authors during the 2001 Fiscal Year. We thank M. Pilch and T. Trucano for reviewing this report.

(Page left blank)

Table of Contents

(Page left blank)

List of Figures

(Page left blank)

List of Tables

(Page left blank)

1.0 Introduction

In the past, numerical models of complex engineered systems were used to provide insight during the design phases rather than to validate the designs. Validation of these designs was accomplished using prototypes and production versions of the resulting engineered systems. As we continue to develop more sophisticated numerical models, our dependence on numerical models has increased while our emphasis on experimental testing at the systems level has decreased. As a result, our need for increased rigor in the assessment of models at the subsystem levels has increased. This requires a more complete understanding of the sources and significance of differences between model predictions and experimental observations and their impact on systems level validity.

This report is the fourth in a series presenting issues related to numerical model validation methodology. In the first report (Hills and Trucano, 1999), the conceptual ideas behind numerical model validation in the presence of experimental and model parameter uncertainty were presented. We discussed the use of statistical methodology to develop model validation metrics for linear and nonlinear models. Examples were presented showing the application of these metrics to several physical applications.

The second report (Hills and Trucano, 2001) further demonstrated the use of these metrics for one-dimensional shock data. We also introduced the idea of a metric that relates the anticipated target application of a model to the measurements taken from validation experiments. This linkage is important since the validation experiments generally do not exactly represent the target application. Validation experiments are typically carefully controlled so that the sources of potential differences between observation and prediction are correctly resolved. For this reason, validation experiments as typically designed to test only a subset of the physics important to the system application. Suites of validation experiments are used to cover the range of physics and the range of anticipated conditions (or parameters) for the target application. Mathematically defining the link between the validation experiments and the target application is important if we wish to provide quantitative evidence as to how well our suite of validation experiments represent the anticipated application of the model. The application-based metric presented in the second report was designed to weight the experimental data so that they better represent the application. More specifically, data that does not have as direct of an impact on the target application was weighted less. This modification uses a sensitivity analysis to define and remove those data (or linear combination of data) from the validation experimental data set for which the target application is not sensitive (see Hills and Trucano, 2001). This has the effect of reducing the impact of such data on the validation metric. An example was presented relating a two-dimensional shock application to the one-dimensional shock physics data used for model validation.

The third report (Hills and Trucano, 2002) focused on the application of the Maximum

Likelihood method to the non-application based validation metrics developed in the first two reports. The use of Maximum Likelihood allows highly nonlinear problems with non-normally distributed uncertainties in the measurements and the model parameters to be more easily analyzed.

The focus of the present work is to further develop the relation between component or unit level validation experiments and more complex and integral system level target applications. Specifically, we investigate the relationship between decision variables that are important to the target application and the measurements obtained from the suite of supporting validation experiments. In this context, we consider a decision variable to be a variable that is important to the application and which is predicted from the model. It is that quantity that defines whether a design is successful. A decision variable may be the temperature in a component, the probability that a component will detonate, or the stress at a critical location. It is not unusual for the decision variable to be different than the quantities measured in the validation experiments. For example, one may not be able to directly measure maximum stress in a component because the location of maximum stress is not accessible.

How do we then tie quantities measured in the validation experiments to the decision variables for the target application and how do uncertainties in these measurements impact our ability to test model validity for the system level predictions? Here we study several approaches. All are based on first order sensitivity analysis. In the first, we look at the sensitivity of the decision variables to the uncertain model parameters, and use the results to define how we should weigh the validation measurements so that linear combinations of the measurements that are not important to the decision variables are given zero weight. This approach is top down in the sense that we modify the validation metric at the unit level, based on a sensitivity analysis of the target application. This approach was introduced in Hills and Trucano (2000a) and will be extended to non-normal distributions in the model parameters.

The remaining approaches look more thoroughly at the relationship between a suite of validation experiments and the target application decision variable. These approaches depend on identifying those model parameters that are important to the target application, be they uncertain or not. The weights for the validation measurements are then determined so that sensitivities of the target application decision variable to the important model parameters are reflected by the weights that are put on the measurements. These approaches are sufficiently general that different levels of uncertainty in the parameters for the models for the experiments, and for the target application, can be accommodated. These approaches also allow us to determine (to first order) whether the validation experiments adequately cover the important physics (represented through the physical parameters) of the target application. While these approaches are conceptually more difficult than the first, they require much of the same information and are not much more difficult to implement. The majority of work presented in this document will focus on these more general approaches.

2.0 Theory

2.1 Background

In this chapter, we develop methodology to relate validation experiments to the target application. The methodology is based on first order sensitivity analysis of the validation experiments and the target application. The analysis is used to provide weights to be applied to the measurements to better represent the application. These weights influence the comparison of model results with experiments and the inferences that can be drawn from them. The first approach presented is an extension of that developed by Hills and Trucano (2001) and is based on projecting the measurements into a subspace relevant to the target application. We call this approach the projection method. Here we extend the projection method to handle non-normal distributions in the model parameters. The second approach provides a more comprehensive look at whether the suite of experiments adequately covers the anticipated application and allows us to evaluate the uncertainty in the resulting application decision variables due to the uncertainty in the model validation measurements. The third approach is similar to the second, but accounts for model parameter uncertainty in developing the weights. We will refer to the second two approaches as representative approaches since we develop the weights so that the resulting linear combinations of measurement best represent the target application. All of these approaches can be used to develop a validation metric (Trucano, et al., 2001). We provide several examples of such metrics. Before we begin the development, we discuss the basic ideas and assumptions behind these approaches.

Figure 2.1 illustrates the basic problem we face. We have some target application for which we wish to test the validity of a model. The model for this application is composed of a system of sub-models which each represent some subset of the physics for the target application. For example, the physics for a target application may include conduction heat transfer, thermal contact resistance, convection, radiation heat transfer, and phase changes. We represent the system level target application by the graphic labeled System in Figure 2.1.

In contrast, we often cannot perform experimental model validation (Trucano, Pilch and Oberkampf, 2002) at the system level due to expense, environmental impact, safety, or simply the inability to run controlled experiments at the system level. In these cases, we must perform validation experiments on sub-system levels that can be accomplished under more carefully controlled and monitored conditions. Here we call these experiments unit level validation experiments. For this approach to work, we must have some assurance that physical testing at the unit level fully represents the physics important at the system level. In terms of the Figure 2.1, the unit level experiments are represented by the building blocks that combine to represent experimental validation of the necessary physics of the target application or system.

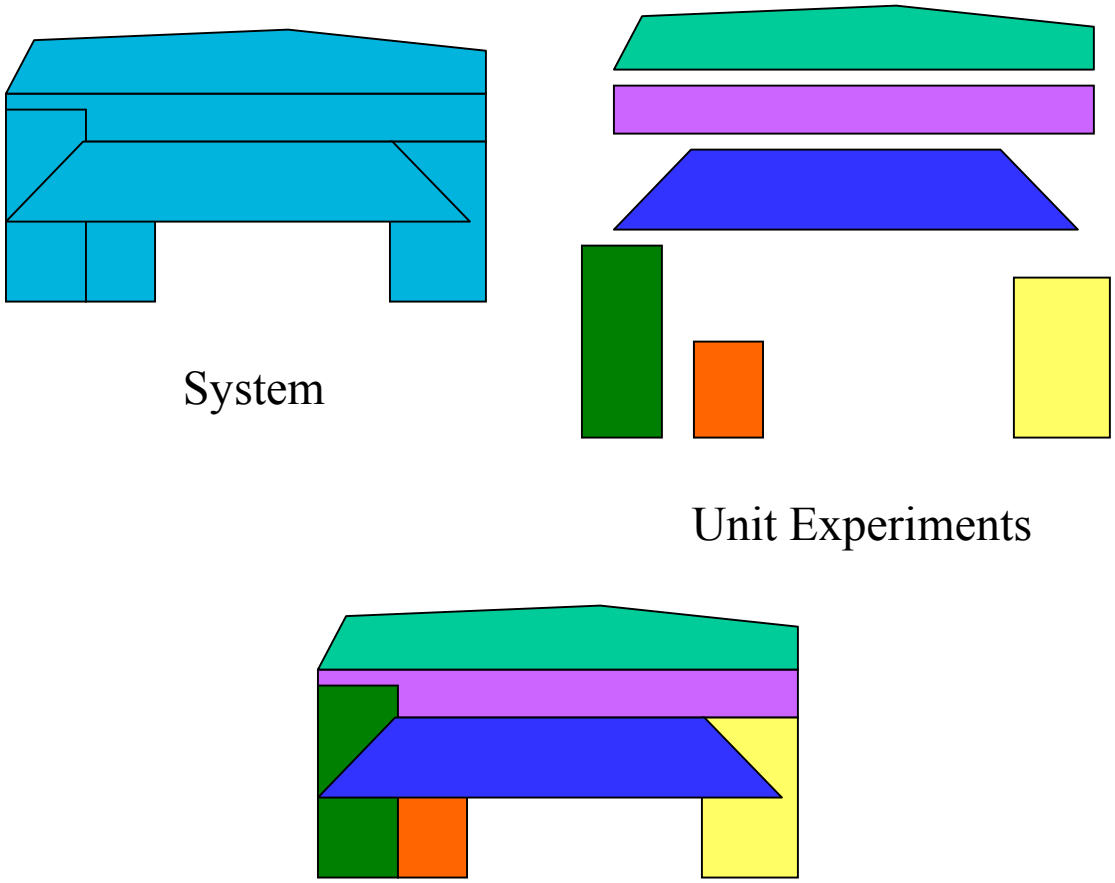

Figure 2.1: Unit to System Level Validation

From the figure, we see that the individual building blocks or unit level validation experiments may not be independent. There may be overlap between several of the unit experiments. For example, it is very difficult to design unit level validation experiments for radiation heat transfer or thermal convection that do not also contain heat conduction. Thus, we may have a suite of unit level validation experiments that all contain some form of heat conduction. The overlap in physics between validation experiments is normal. However, we do want our unit level experiments to combine to cover all of the physics deemed relevant to our target application. In terms of Figure 2.1, this is represented by "Combined Results." We do not want any holes in the graphic labeled Combined Results.

A second issue that we must deal with is to decide how the data from the unit level experiments should be combined to best assess the validity of the model for our target application. If the performance of the model for the target application is especially

sensitive to a particular sub-physics, say thermal radiation, then we expect that we may want to weight the results from the thermal radiation validation experiments more heavily. We also want to know what level of uncertainty we can tolerate in the validation experiments (both in the measurements and in the model parameters) so that the results remain useful for a target application validation.

Figure 2.2 illustrates issues related to uncertainty. We begin with the part of the figure labeled Unit Experiments. Note that we show probability density clouds for both the uncertainty in the model parameters α used to model the validation experiment or experiments, and the uncertainty in the measurements γ. Once we define a procedure to combine these experiments to best reflect the target application, we would like to estimate what the corresponding uncertainty is in the target application, based on our models for the system physics and the uncertainties in the validation measurements and the parameters. We wish this uncertainty to be less than the acceptable uncertainty in the target application. If, in fact, the uncertainty is larger in our combined results for the target application than is acceptable for the target application, then clearly our validation experiments are not of sufficient resolution to support our target application validation. The system level target application is also shown in Figure 2.2. We denote the critical target application predicted decision variable by d. This variable may be a scalar or a vector. Note that we have included the uncertainty in the system model parameters and shown the effect of the uncertainty in d (a scalar in this case). We have also shown the uncertainty in the model parameters for the unit experiments and the measurements, and included the effect in the combined results for the decision variable d. We intentionally showed the uncertainty (represented by the spread in the depicted probability density function for d) in the model parameters for the unit/validation experiments as less than for the application. Generally, we can more carefully control (hence less uncertainty) these parameters for the model validation experiments than we can for the application. This is desirable because we want the combined results from the unit experiments to have less uncertainty (narrower PDF) than the acceptable level of uncertainty for the target application as a basic principle for designing unit validation experiments.

How do we address the above issues? Here we develop several approaches based on a first order sensitivity analysis for the models for the validation experiments and for the target application. While these approaches do have limitations for highly nonlinear problems where we expect to have to go beyond first order sensitivity analysis, they do represent a very good first step that can be implemented within the current framework of software development at Sandia National Laboratories. We suggest that accounting for this linkage between the unit level experiments and the target application, to first order, is much more desirable than not accounting for this linkage at all. The first order analysis will insure that the physics that the sensitivity analysis tells us is more important to the target application will be given greater weight in the analysis.

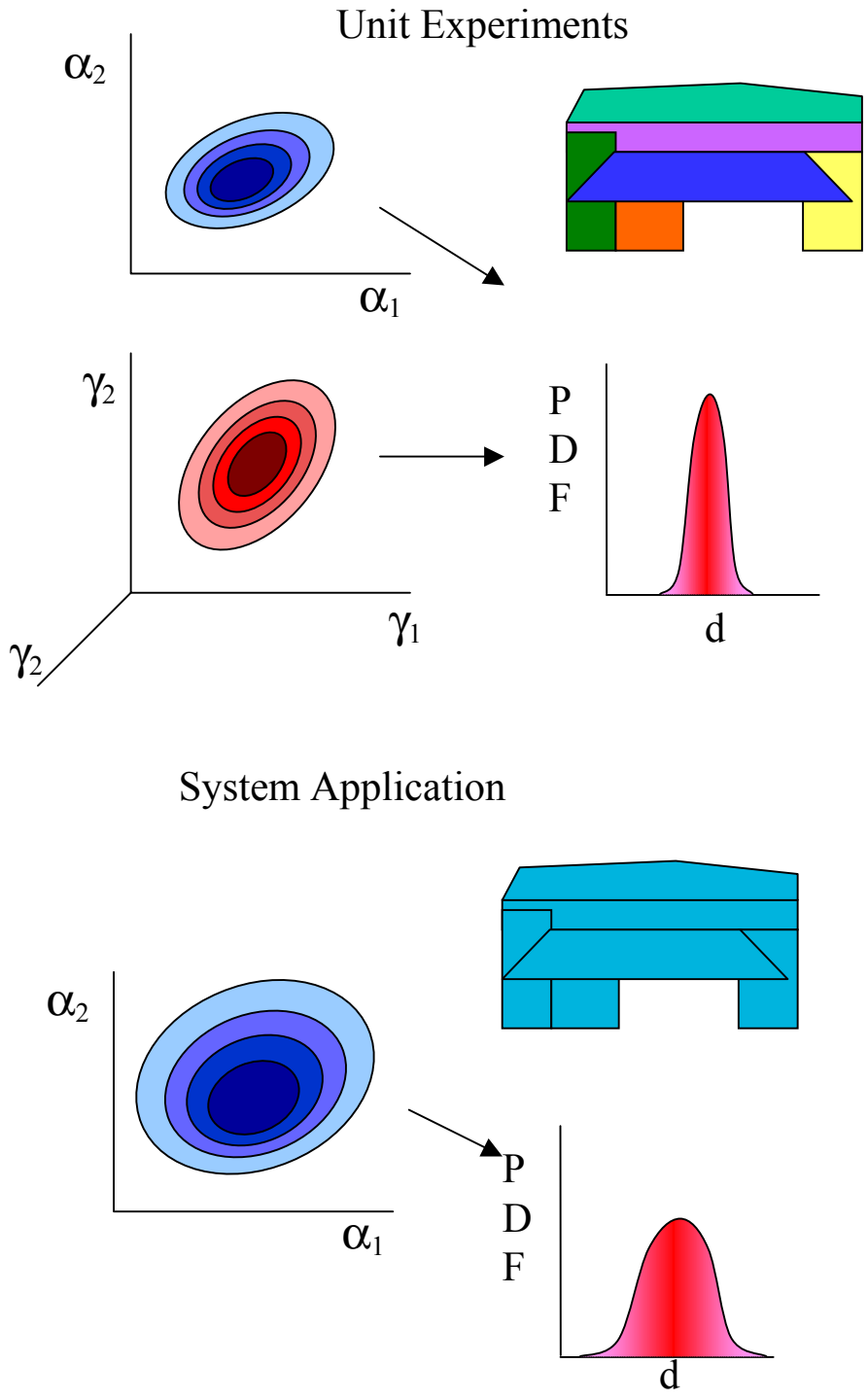

Figure 2.2: Uncertainty in Unit to System Level Validation

2.2 Theory

We begin with a list of assumptions common to all three approaches.

1. We assume that it is practical to perform first order uncertainty analysis of the system level application and each of the unit level validation experiments for the important model parameters (i.e., those whose effect on the application is believed to be significant).

2. We assume that a representation of first order dependencies between various physical phenomena is adequate at the unit level to represent the target application. If we have a zero first order sensitivity, but a non-zero second order sensitivity, then the present analysis will not properly account for this dependence.

3. We assume that we have adequate characterization of the uncertainty in the experimental measurements for the validation experiments. Specifically, we assume that we know the form of the probability distribution, and have estimated values of all of the statistical parameters for the measurements except the statistic describing central tendency of the distribution (i.e., mean, median, mode). This assumption is required late in the analysis for the development of a validation metric. This assumption is not required for the first order sensitivity analysis, which addresses coverage of the target application by the unit level experiments and estimates the covariance of the reconstructed decision variable.

The effect of uncertainty in the model parameters is ignored in the first and second approaches we discuss to evaluate the measurement weights. This uncertainty will be accounted for by a third approach. We begin with our model for the target application:

$$\mathbf{d} = \mathbf{G}(\boldsymbol{\alpha}) \tag{2.1}$$

where $\mathbf{d}$ is a vector of decision variables, G is a model for the target application, and $\boldsymbol{\alpha}$ are the important model parameters and/or calibration parameters and/or important model quantities (see discussion below).

A decision variable for the target application is a model predicted quantity critical to the success of the target application, i.e., a variable that we use to decide whether the target system was successful at meeting its design goal. Examples include temperature in a temperature sensitive critical component, depth of penetration of a projectile, or the probability of detonation of an explosive device. Note that a decision variable for a target application may or may not correspond to the quantities measured during validation experiments. For example, we may measure the velocity of a foam thermal decomposition front in a one-dimensional experiment whereas we may really be interested in the thermal protection afforded by the foam on a component in a system. While front speed

measurements are a good indicator of the predictive ability of a model, and can be measured non-invasively using radiography, they are not a direct measure of the thermal environment of the component. However, front speed measurement may be a very appropriate measure if the location of the front (or the arrival time of the front at the component) significantly impacts the thermal environment of the component.

Our target application is the particular (complex) system to which we will apply our model. In (2.1), we represent this model as a function of the vector of important model parameters and/or calibration parameters and/or parameterization of important model quantities $\boldsymbol{\alpha}$. We consider the model parameters as those parameters that appear in our constitutive models for the application, for example. Whereas, we consider the calibration parameters as those parameters that may appear in non-physics based correction calibrations for sub-models. We also extend this latter definition to include parameterization of important model quantities that are important to the target application but not represented by the collection of model parameters. Note that in most cases, it is a practical consideration that our constitutive parameters are also obtained from calibration procedures and therefore also often possess uncertainty. While there may be differences in the source of the various parameters, the methods presented here allow for similar treatment, and we show both of these parameter types as components in the single parameter vector $\boldsymbol{\alpha}$.

We are now ready to write a expression similar to (2.1) for our unit level validation measurements. We write the model predictions for a set of unit level measurements as

$$\boldsymbol{\gamma} = \mathbf{F}(\boldsymbol{\alpha}) \tag{2.2}$$

where $\boldsymbol{\gamma}$ represents the prediction vector of validation measurements from a suite of experiments. We emphasize that these measurements may be from suites of experiments that involve different experimental apparatus. Each suite may test the model for different physics. $\mathbf{F}$ represents a vector of models for the various validation experiments and $\boldsymbol{\alpha}$ a vector of model parameters. We intentionally and reasonably use the same vector for the parameters in Eq. (2.2) as we did in (2.1). Note that the vector of parameters $\boldsymbol{\alpha}$ in Eq. (2.1) represents the vector of all parameters of significance to the target application. If our validation experiments span the physics of the target application, then we should expect that all of the model parameters of importance to the target application will also be important in the suite of validation experiments. In addition, we may expect that individual validation experiments may not be sensitive to the full set of model parameters, but desire the suite of validation experiments to be defined such that they cover the entire set of parameters as required for the target application.

The vector of model parameters is important to the present development since it provides the linkage to relate the validation experiments to the target application. The choice of which parameters to include in this set will require judgment.

We desire to weight the unit validation experimental data to best represent the target application. Here we evaluate the weighting through a first order sensitivity analysis. We begin by applying a Taylor's series expansion to Eq. (2.1) and retaining the first order terms.

$$\Delta \mathbf{d} \approx \nabla_{\alpha} \mathbf{G}(\boldsymbol{\alpha}) \Delta \boldsymbol{\alpha} \tag{2.3}$$

The gradient term is evaluated at the anticipated values for the target application. Repeating this process for Eq. (2.1) gives

$$\Delta \boldsymbol{\gamma} \approx \nabla_{\alpha} \mathbf{F}(\boldsymbol{\alpha}) \Delta \boldsymbol{\alpha} \tag{2.4}$$

At this point, we can take two approaches. Both approaches are based on evaluating weights of the measurement data to better represent the target application. The first, based on that presented by Hills and Trucano (2001), is to look at those directions in the validation space that are not important to the decision variable, and remove the effect of these directions. Here we extend this approach to non-Gaussian model parameters. The second approach is to take that weighted combination of the measurement data that best represents the decision variable for the target application. The second approach not only throws out non-important directions in the validation space, but it also weights the remaining directions in a fashion appropriate to the target application decision variable. We begin with the first approach.

2.2.1 Projection Method

In this development, we restrict our attention to a single decision variable. For this case, we rewrite Eq. (2.3) as

$$\Delta d \approx \mathbf{g}^{\mathrm{T}} \Delta \boldsymbol{\alpha} \tag{2.5}$$

where

$$\mathbf{g} = \left(\nabla_{\alpha} \mathbf{G}(\boldsymbol{\alpha})\right)^{\mathrm{T}} \tag{2.6}$$

We would like to determine those directions in the parameter space that are not important to the decision variable. Denote this direction by **b** and require that **b** satisfy the following:

$$\Delta \mathrm{d} \approx \mathbf{g}^{\mathrm{T}} \mathbf{b} = 0 \tag{2.7}$$

We see that **b** is orthogonal to the sensitivity vector **g** for the target application. This direction is illustrated conceptually in the upper right part of Figure 2.3. While the direction of **b** is uniquely defined by Eq. (2.7) (assuming **g** is non-zero), the magnitude of **b** is arbitrary. Since **b** will be normalized later, the choice of magnitude of **b** is arbitrary at

this stage in the development. Given a **b**, we can map this direction into validation space using the sensitivity matrix found previously for the validation experiments.

$$\boldsymbol{\beta} = \nabla_{\alpha}\mathbf{F}\ \mathbf{b} = \mathbf{X}\mathbf{b} \tag{2.8}$$

This direction is illustrated conceptually in the lower part of Figure 2.3. Since discrepancies between the model predictions and the experimental observations do not have an impact on the application decision variable along this direction, we do not need to measure the prediction-measured differences along this direction. To remove this direction, we project the validation space into a hyperplane orthogonal to $\boldsymbol{\beta}$. The projection matrix that projects points in the *n*-dimensional space into the desired *n*-1 dimensional hyperplane is given by (Strang, 1976)

$$\mathbf{P} = \mathbf{I} - \boldsymbol{\beta}(\boldsymbol{\beta}^{\mathsf{T}}\boldsymbol{\beta})^{-1}\boldsymbol{\beta}^{\mathsf{T}} \tag{2.9}$$

where **I** is the identity matrix. Note that application of the above projection to $\boldsymbol{\beta}$ itself (or some multiple of $\boldsymbol{\beta}$) should result in zero:

$$\begin{aligned} \mathbf{P}\boldsymbol{\beta} &= (\mathbf{I} - \boldsymbol{\beta}(\boldsymbol{\beta}^{\mathsf{T}}\boldsymbol{\beta})^{-1}\boldsymbol{\beta}^{\mathsf{T}})\boldsymbol{\beta} \\ &= \boldsymbol{\beta} - \boldsymbol{\beta}(\boldsymbol{\beta}^{\mathsf{T}}\boldsymbol{\beta})^{-1}(\boldsymbol{\beta}^{\mathsf{T}}\boldsymbol{\beta}) \\ &= \boldsymbol{\beta} - \boldsymbol{\beta} = \mathbf{O} \end{aligned} \tag{2.10}$$

We see that this subspace ignores the direction in the *n*-dimensional validation space that corresponded to no change in the application decision variable. We can now use the projection **P** to project quantities in our *n* dimensional validation space into the *n*-1 subspace,

$$\boldsymbol{\gamma}^{\mathrm{p}} = \mathbf{P}\ \boldsymbol{\gamma} \tag{2.11}$$

where the p superscript denotes a projection into the subspace. This projection was developed in Hills and Trucano (2001) and was demonstrated using shock physics data. This projection weights the measurements so that the directions in the validation space (at least to first order) that are not important to the decision variable are ignored. In the following section, we extend this development to not only ignore the non-important directions, but to weight the remaining directions to best reflect the application.

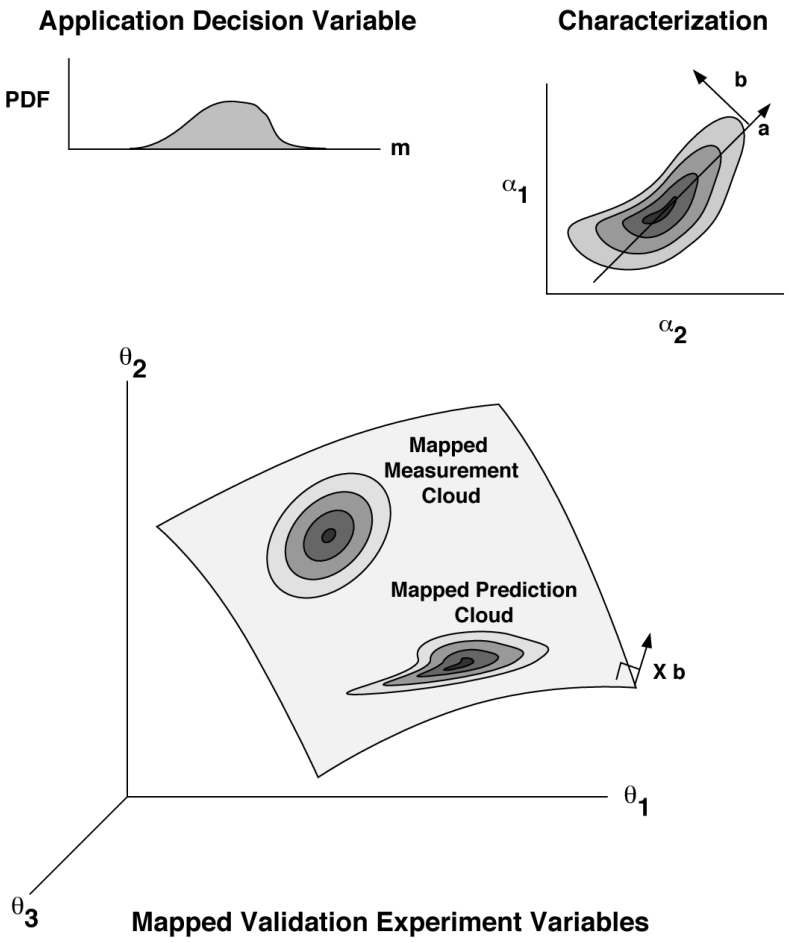

Figure 2.3: Model Validation Sub-Space as Defined by an Application Decision Variable

2.2.2 Representative Method: Uncertainty in Measurement Only

Our second (and third) approach not only ignores those directions in the validation space that are not important to the system level target application, but also weights the remaining directions relative to their importance. We do this by choosing the weights for the vector of measurements from the validation experiments so that they have the same sensitivity to the important model parameters $\boldsymbol{\alpha}$ as do the target decision variables. We denote this weighting matrix by **A** (to contrast it from the **P** matrix defined in the previous section) and require the following:

$$\mathbf{A}^T \Delta\boldsymbol{\gamma} \approx \Delta\mathbf{d} \tag{2.12}$$

So (see Eqs. (2.3) and (2.4))

$$\mathbf{A}^T \nabla_{\alpha}\mathbf{F}(\boldsymbol{\alpha})\Delta\boldsymbol{\alpha} \approx \nabla_{\alpha}\mathbf{G}(\boldsymbol{\alpha})\Delta\boldsymbol{\alpha} \tag{2.13}$$

or

$$\left((\nabla_{\alpha}\mathbf{F}(\boldsymbol{\alpha}))^T \mathbf{A} - (\nabla_{\alpha}\mathbf{G}(\boldsymbol{\alpha}))^T\right)^T \Delta\boldsymbol{\alpha} \approx \mathbf{0} \tag{2.14}$$

Since $\Delta\boldsymbol{\alpha}$ can take on any value (i.e., we have not restricted $\Delta\boldsymbol{\alpha}$ to a particular direction), we must have that

$$(\nabla_{\alpha}\mathbf{F}(\boldsymbol{\alpha}))^T \mathbf{A} \approx (\nabla_{\alpha}\mathbf{G}(\boldsymbol{\alpha}))^T \tag{2.15}$$

Note that the above equation defines the weighting matrix **A** such that the weighted measurements and the decision variable have the same sensitivity to the important model parameters. Solving for **A**, we can write the covariance of $\Delta\mathbf{d}$ in terms of the covariance matrix of $\Delta\boldsymbol{\gamma}$ (see Hills and Trucano, 2000a):

$$\text{cov}(\mathbf{d}) = \mathbf{A}^T \text{cov}(\boldsymbol{\gamma})\, \mathbf{A} \tag{2.16}$$

Equations (2.15) and (2.16) provide us with the following 3 pieces of important information. First, for the left and right sides of Eq. (2.15) to be similar, the rows of $\nabla_{\alpha}\mathbf{F}(\boldsymbol{\alpha})$ must span the rows of $\nabla_{\alpha}\mathbf{G}(\boldsymbol{\alpha})$. In other words, the sensitivity of the unit level validation experiments to the parameters $\boldsymbol{\alpha}$ must span the target application sensitivity to the same parameters. If we have an incomplete set of validation experiments, then rows of $\nabla_{\alpha}\mathbf{F}(\boldsymbol{\alpha})$ will not span the target application. Secondly, Eq. (2.15) tells us in part how to estimate **A**, the weighting of our unit level measurements, so that the weighted measurements have the same sensitivity to the important model parameters as the decision variable. Finally, given an estimate of **A**, we can use Eq. (2.16) to evaluate the sensitivity of our reconstructed decision variable at the system level to small changes in our measurements. More specifically, this expression allows us to evaluate whether the uncertainty in the validation experiments is sufficiently low to resolve the validity of the

systems level model for the target application. These observations are best demonstrated through the examples in the following chapter.

How do we actually evaluate the weighting matrix **A**? Note that in most cases, the number of model parameters will be different than the number of measurements. Thus, the matrix on the left hand side of Eq. (2.15) will not be square. For the case of fewer independent measurements than model parameters, the matrix on the left hand side will generally not span the space required to represent the right hand side. In other words, our validation experiments do not have sufficient data of the right type to represent the target application as discussed previously. In this case, we cannot proceed further. We have to instead reconsider the design of the validation experiments. Another case is when we have more measurements than model parameters. For this case, we will have more unknown weights than we have equations and Eq. (2.15) is underconstrained. There are an infinity of weighting vectors (or matrices) that lead to solutions of Eq. (2.15). How do we choose a desirable solution? Eq. (2.16) provides us some guidance. Since we wish to maximize our ability to resolve the decision variable for the target application, we should choose the solution from the infinity of solutions that minimizes the uncertainty in the reconstructed decision variable or variables defined by the covariance given by Eq. (2.16).

First, consider a single decision variable *d* (or a component in a vector of decision variables). Eqs. (2.15) and (2.16) become

$$(\nabla_{\boldsymbol{\alpha}}\mathbf{F}(\boldsymbol{\alpha}))^{\mathrm{T}}\,\mathbf{a} \approx \mathbf{g} \tag{2.17}$$

$$\sigma_d^2 = \mathbf{a}^{\mathrm{T}}\,\mathrm{cov}(\boldsymbol{\gamma})\,\mathbf{a} \tag{2.18}$$

where

$$(\nabla_{\boldsymbol{\alpha}}\mathbf{G}(\boldsymbol{\alpha}))^{\mathrm{T}} = \mathbf{g} \tag{2.19}$$

Note that we replaced the cov(**d**) in Eq. (2.16) with variance of d (i.e., square of the standard deviation) since we are considering a single decision variable. Note that **A** and $\nabla_{\boldsymbol{\alpha}}\mathbf{G}(\boldsymbol{\alpha})$ are now vectors (denoted by **a** and **g**) since we are dealing with a single decision variable. We wish to choose **a** such that σ_d^2 is minimized, given the constraint defined by Eq. (2.17). To accomplish this constrained minimization, we use a vector of Lagrange multipliers $\boldsymbol{\lambda}$ as follows. Find the **a** and $\boldsymbol{\lambda}$ that minimizes

$$\min L = \mathbf{a}^{\mathbf{T}}\,\mathrm{cov}(\boldsymbol{\gamma})\,\mathbf{a} + \boldsymbol{\lambda}^{\mathrm{T}}\left((\nabla_{\boldsymbol{\alpha}}\mathbf{F}(\boldsymbol{\alpha}))^{\mathrm{T}}\,\mathbf{a} - \mathbf{g}\right) \tag{2.20}$$

Note that since we are taking Eq. (2.17) to be true, the **a** and $\boldsymbol{\lambda}$ that minimizes Eq. (2.20) also minimizes Eq. (2.18). The minimum occurs at

$$\nabla_{\mathbf{a}} L = 0 = \mathrm{cov}(\boldsymbol{\gamma})\,\mathbf{a} + (\nabla_{\boldsymbol{\alpha}}\mathbf{F}(\boldsymbol{\alpha}))\,\boldsymbol{\lambda} \tag{2.21}$$

So

$$\mathbf{a} = \left(\text{cov}(\boldsymbol{\gamma})\right)^{-1} \left(\nabla_{\boldsymbol{\alpha}} \mathbf{F}(\boldsymbol{\alpha})\right) \boldsymbol{\lambda} \tag{2.22}$$

Using (2.22) in (2.17) gives (assuming an equality)

$$\left(\nabla_{\boldsymbol{\alpha}} \mathbf{F}(\boldsymbol{\alpha})\right)^{\mathrm{T}} \left(\text{cov}(\boldsymbol{\gamma})\right)^{-1} \left(\nabla_{\boldsymbol{\alpha}} \mathbf{F}(\boldsymbol{\alpha})\right) \boldsymbol{\lambda} = \mathbf{g} \tag{2.23}$$

So

$$\boldsymbol{\lambda} = \left(\left(\nabla_{\boldsymbol{\alpha}} \mathbf{F}(\boldsymbol{\alpha})\right)^{\mathrm{T}} \left(\text{cov}(\boldsymbol{\gamma})\right)^{-1} \left(\nabla_{\boldsymbol{\alpha}} \mathbf{F}(\boldsymbol{\alpha})\right)\right)^{-1} \mathbf{g} \tag{2.24}$$

Note that if the validation experiments do not span the space of the target application decision variable, then the inverse of the product of the three matrices in Eq. (2.24) will not exist. Using (2.24) in (2.22) gives

$$\mathbf{a} = \left(\text{cov}(\boldsymbol{\gamma})\right)^{-1} \left(\nabla_{\boldsymbol{\alpha}} \mathbf{F}(\boldsymbol{\alpha})\right) \left(\left(\nabla_{\boldsymbol{\alpha}} \mathbf{F}(\boldsymbol{\alpha})\right)^{\mathrm{T}} \left(\text{cov}(\boldsymbol{\gamma})\right)^{-1} \left(\nabla_{\boldsymbol{\alpha}} \mathbf{F}(\boldsymbol{\alpha})\right)\right)^{-1} \mathbf{g} \tag{2.25}$$

Eq. (2.25) represents the weighting of the validation measurements that minimizes the variance of the reconstructed decision variable. We can use Eq. (2.25) to find an **a** for each decision variable *d* in a vector of decision variables. Thus, we can handle a vector of decision variables, component by component as follows (see Eqn. (2.19)):

$$\mathbf{A} = \left(\text{cov}(\boldsymbol{\gamma})\right)^{-1} \left(\nabla_{\boldsymbol{\alpha}} \mathbf{F}(\boldsymbol{\alpha})\right) \left(\left(\nabla_{\boldsymbol{\alpha}} \mathbf{F}(\boldsymbol{\alpha})\right)^{\mathrm{T}} \left(\text{cov}(\boldsymbol{\gamma})\right)^{-1} \left(\nabla_{\boldsymbol{\alpha}} \mathbf{F}(\boldsymbol{\alpha})\right)\right)^{-1} \left(\nabla_{\boldsymbol{\alpha}} \mathbf{G}(\boldsymbol{\alpha})\right)^{\mathrm{T}} \tag{2.26}$$

2.2.3 Representative Method: Uncertainty in Measurements and Model Parameters

Here we repeat the previous development, but explicitly account for uncertainty in the model parameters for the validation experiments and for the target application. We begin by expanding the argument list of Eq. (2.1) and (2.2) to account for uncertainty in the model parameters.

$$\boldsymbol{\gamma} = \mathbf{F}(\boldsymbol{\alpha}, \boldsymbol{\alpha}_v) \tag{2.27}$$

where $\boldsymbol{\alpha}$ represents the model parameters that represent the important physics that one wishes to capture in the target application, and $\boldsymbol{\alpha}_v$ represents the model parameters that contain uncertainty (treated as random variables). $\boldsymbol{\alpha}$ and $\boldsymbol{\alpha}_v$ may be vectors of the same parameters, different parameters, or some of each. The lengths of these two vectors need not be the same. Note that components in both of these vectors may represent the same parameter. In this case (i.e. a parameter represents important physics and contains uncertainty), we can take $\boldsymbol{\alpha}$ as an expected value and $\boldsymbol{\alpha}_v$ as a perturbation from the

expected value due to uncertainty. This allows us to separate the sensitivity of a model prediction to a parameter that represents physics (e.g., the impact thermal conductivity has on a temperature measurement) and the sensitivity of this parameter to uncertainty in this parameter. This distinction is important if we wish to represent the sensitivity of the model prediction to the parameter (important if we are to represent the physics), whether or not the parameter is uncertain. Note that for the case of an important model parameter possessing uncertainty, the expected value of $\boldsymbol{\alpha}_v$ is zero since $\boldsymbol{\alpha}_v$ represents a perturbation due to uncertainty from the expected value of $\boldsymbol{\alpha}$.

We write a similar expression for the target application model.

$$\mathbf{d} = \mathbf{G}(\boldsymbol{\alpha}, \boldsymbol{\alpha}_a) \tag{2.28}$$

$\boldsymbol{\alpha}_v$ and $\boldsymbol{\alpha}_a$ may be different vectors of different lengths. We do not require the uncertain parameters to be the same for the validation experiments and the target application. Even if the same parameters are uncertain in both cases, the uncertainties will generally be different since validation experiments typically are more carefully controlled. We will provide an example in the next chapter of a case where the uncertainties in the model parameters are greater for the target application than they are for the model validation experiments.

We now apply a first order sensitivity analysis

$$\Delta\boldsymbol{\gamma} \approx \nabla_{\boldsymbol{\alpha}}\mathbf{F}(\boldsymbol{\alpha}, \boldsymbol{\alpha}_v)\Delta\boldsymbol{\alpha} + \nabla_{\boldsymbol{\alpha}_v}\mathbf{F}(\boldsymbol{\alpha}, \boldsymbol{\alpha}_v)\Delta\boldsymbol{\alpha}_v \tag{2.29}$$

$$\Delta\mathbf{d} \approx \nabla_{\boldsymbol{\alpha}}\mathbf{G}(\boldsymbol{\alpha}, \boldsymbol{\alpha}_a)\Delta\boldsymbol{\alpha} + \nabla_{\boldsymbol{\alpha}_a}\mathbf{G}(\boldsymbol{\alpha}, \boldsymbol{\alpha}_a)\Delta\boldsymbol{\alpha}_a \tag{2.30}$$

and take a weighted combination of the predicted measurements to best represent the target application.

$$\begin{aligned}&\mathbf{A}^{\mathrm{T}}\nabla_{\boldsymbol{\alpha}}\mathbf{F}(\boldsymbol{\alpha}, \boldsymbol{\alpha}_v)\Delta\boldsymbol{\alpha} + \mathbf{A}^{\mathrm{T}}\nabla_{\boldsymbol{\alpha}_v}\mathbf{F}(\boldsymbol{\alpha}, \boldsymbol{\alpha}_v)\Delta\boldsymbol{\alpha}_v \\ &= \nabla_{\boldsymbol{\alpha}}\mathbf{G}(\boldsymbol{\alpha}, \boldsymbol{\alpha}_a)\Delta\boldsymbol{\alpha} + \nabla_{\boldsymbol{\alpha}_a}\mathbf{G}(\boldsymbol{\alpha}, \boldsymbol{\alpha}_a)\Delta\boldsymbol{\alpha}_a\end{aligned} \tag{2.31}$$

As discussed in the paragraph following Eq. (2.27), we take $\boldsymbol{\alpha}$ as expected values and $\boldsymbol{\alpha}_v$ and $\boldsymbol{\alpha}_a$ as perturbations from the expected values due to uncertainty. Taking the expected value of Eq. (2.31) leads to

$$\left(\nabla_{\boldsymbol{\alpha}}\mathbf{F}(\boldsymbol{\alpha}, \boldsymbol{\alpha}_v)\right)^{\mathrm{T}}\mathbf{A} = \left(\nabla_{\boldsymbol{\alpha}}\,\mathbf{G}(\boldsymbol{\alpha}, \boldsymbol{\alpha}_a)\right)^{\mathrm{T}} \tag{2.32}$$

since the expected value of a random perturbation from its expected value is zero and since we hold the gradient terms at fixed values for the parameters (i.e., a first order analysis). Note that Eq. (2.32) is the same as Eq. (2.15). For the case that the columns of the gradient term of the left hand side of Eq. (2.32) do not span the space of the columns

of the right side, the validation experiments do not span the space of the target application decision variables. For the case that there are as many parameters as unknowns with the rank of the left hand gradient matrix equal to the number of unknowns, a unique **A** exists.

$$\mathbf{A} = \left(\left(\nabla_{\boldsymbol{\alpha}} \mathbf{F}(\boldsymbol{\alpha}, \boldsymbol{\alpha}_v) \right)^{\mathrm{T}} \right)^{-1} \left(\nabla_{\boldsymbol{\alpha}} \mathbf{G}(\boldsymbol{\alpha}, \boldsymbol{\alpha}_a) \right)^{\mathrm{T}} \tag{2.33}$$

The remaining case is when the left matrix does span the space of the RHS, but we have more measurements than model parameters. In this case, the system is underconstrained and we have the opportunity for additional constraints. As in the previous section, we will choose the **A** that satisfies Eq. (2.32) while minimizing the uncertainty in the reconstructed decision variable sensitivity as measured by the variance. This has the effect of maximizing our sensitivity to uncertainty in the differences between model predictions and experimental observations, weighted in a fashion appropriate for the decision variable. As before, we accomplish this through Lagrange multipliers. We minimize the following:

$$\min L = \mathbf{A}^{\mathbf{T}} \operatorname{cov}(\mathbf{F} - \boldsymbol{\gamma}) \mathbf{A} + \boldsymbol{\lambda}^{\mathrm{T}} \left(\left(\nabla_{\boldsymbol{\alpha}} \mathbf{F}(\boldsymbol{\alpha}, \boldsymbol{\alpha}_v) \right)^{\mathrm{T}} \mathbf{A} - \nabla_{\boldsymbol{\alpha}} \mathbf{G}(\boldsymbol{\alpha}, \boldsymbol{\alpha}_v) \right)^{\mathrm{T}} \tag{2.34}$$

Using the procedures presented in the previous section leads to the following (see Eq. (2.26)):

$$\begin{aligned} \mathbf{A} = & \left(\operatorname{cov}(\mathbf{F} - \boldsymbol{\gamma}) \right)^{-1} \left(\nabla_{\boldsymbol{\alpha}} \mathbf{F}(\boldsymbol{\alpha}, \boldsymbol{\alpha}_v) \right) \\ & \left(\left(\nabla_{\boldsymbol{\alpha}} \mathbf{F}(\boldsymbol{\alpha}, \boldsymbol{\alpha}_v) \right)^{\mathrm{T}} \left(\operatorname{cov}(\mathbf{F} - \boldsymbol{\gamma}) \right)^{-1} \left(\nabla_{\boldsymbol{\alpha}} \mathbf{F}(\boldsymbol{\alpha}, \boldsymbol{\alpha}_v) \right) \right)^{-1} \left(\nabla_{\boldsymbol{\alpha}} \mathbf{G}(\boldsymbol{\alpha}, \boldsymbol{\alpha}_a) \right)^{\mathrm{T}} \end{aligned} \tag{2.35}$$

where the covariance in the differences between the model predictions and the experimental observations is approximated by (see Hills and Trucano (1999))

$$\operatorname{cov}(\mathbf{F} - \boldsymbol{\gamma}) = \operatorname{cov}(\boldsymbol{\gamma}) + \nabla_{\alpha_v} \mathbf{F}(\boldsymbol{\alpha}, \boldsymbol{\alpha}_v) \operatorname{cov}(\boldsymbol{\alpha}_v) \nabla_{\alpha_v} \mathbf{F}(\boldsymbol{\alpha}, \boldsymbol{\alpha}_v)^{\mathrm{T}} \tag{2.36}$$

Given the **A** defined by Eq. (2.35), we can evaluate the uncertainty in the reconstructed decision variable difference as follows. Take the resulting $\mathbf{A}^{\mathrm{T}}$ times Eq. (2.29), and using the results in Eqs. (2.30) and (2.31), gives

$$\Delta \mathbf{d} \approx \mathbf{A}^{\mathrm{T}} \Delta \boldsymbol{\gamma} - \mathbf{A}^{\mathrm{T}} \nabla_{\alpha_v} \mathbf{F}(\boldsymbol{\alpha}, \boldsymbol{\alpha}_v) \Delta \boldsymbol{\alpha}_v + \nabla_{\boldsymbol{\alpha}_a} \mathbf{G}(\boldsymbol{\alpha}, \boldsymbol{\alpha}_a) \Delta \boldsymbol{\alpha}_a \tag{2.37}$$

Eq. (2.37) can be written as

$$\Delta \mathbf{d} \approx \begin{bmatrix} \mathbf{A}^{\mathrm{T}} & -\mathbf{A}^{\mathrm{T}} \nabla_{\alpha_v} \mathbf{F}(\boldsymbol{\alpha}, \boldsymbol{\alpha}_v) & \nabla_{\boldsymbol{\alpha}_a} \mathbf{G}(\boldsymbol{\alpha}, \boldsymbol{\alpha}_a) \end{bmatrix} \begin{bmatrix} \Delta \boldsymbol{\gamma} \\ \Delta \boldsymbol{\alpha}_v \\ \Delta \boldsymbol{\alpha}_a \end{bmatrix} \tag{2.38}$$

Assume that our uncertainties in the measurements are independent of the uncertainties in the validation model parameters, which in turn, are independent of the uncertainties in the target application model parameters. In this case, we can estimate the total uncertainty in the decision variable for the reconstructed model as follows:

$$\begin{aligned} \mathrm{cov}(\mathbf{d}) = \mathbf{A}^{\mathrm{T}}\,\mathrm{cov}(\boldsymbol{\gamma})\mathbf{A} + \mathbf{A}^{\mathrm{T}}\nabla_{\boldsymbol{\alpha}_v}\mathbf{F}(\boldsymbol{\alpha},\boldsymbol{\alpha}_v)\,\mathrm{cov}(\boldsymbol{\alpha}_v)(\mathbf{A}^{\mathrm{T}}\nabla_{\boldsymbol{\alpha}_v}\mathbf{F}(\boldsymbol{\alpha},\boldsymbol{\alpha}_v))^{\mathrm{T}} \\ + \nabla_{\boldsymbol{\alpha}_a}\mathbf{G}(\boldsymbol{\alpha},\boldsymbol{\alpha}_a)\,\mathrm{cov}(\boldsymbol{\alpha}_a)(\nabla_{\boldsymbol{\alpha}_a}\mathbf{G}(\boldsymbol{\alpha},\boldsymbol{\alpha}_a))^{\mathrm{T}} \end{aligned} \tag{2.39}$$

Eq. (2.39) defines the uncertainty in the reconstructed decision variable vector; given the uncertainty the model parameters for the validation experiments, the uncertainty in the model parameters for the target application, and the uncertainty in the validation measurements. Note that the last term in Eq. (2.39) represents the uncertainty in the target application model prediction of the decision variable. Thus, the uncertainty in the reconstructed variable will be greater due the added uncertainties in the validation measurements and in the model parameters for the validation models.

2.3 Validation

The previous development uses first order sensitivity analysis to weight the measurements to better represent the target application decision variables. The only assumptions we made as to the structure of the uncertainty is the covariance matrices for the measurements, validation model parameters, and application model parameters are known; and the first and second moments of all probability density functions considered (i.e., expected value and variances) exist. We have not assumed functional forms for the probability density functions up to this point.

How should we use this development to define validation metrics that best reflect the application? Before we go further, we make the following observations:

1. The acceptable level of uncertainty in the target application decision variables should be a significant factor in defining validation metrics. Here we focus on a specific application over a limited range of operational conditions and do not address the validity of the model for all possible applications.

2. The sensitivity of the target application decision variables to the validation experiments should be explicitly accounted for. For example, if our target application is much more sensitive to forced heat convection in a certain parameter range than it is to radiation heat transfer, we should weigh the results from the validation experiments that address heat convection in that parameter range more heavily. Furthermore, the sensitivity of the reconstructed decision variables to particular validation experimental measurements should be used to evaluate whether the validation experiments are performed at sufficient accuracy

to resolve the reconstructed decision variable relative to the acceptable level of uncertainty for the target application. The representative approach developed in previous sections allows us to do this.

3. If we can define an acceptable level of uncertainty in the reconstructed decision variables, then we have some flexibility in defining acceptable levels of uncertainty over the suite of validation experiments. For example, we may find that if somewhat uncertain validation experiments are accompanied by validation experiments with little uncertainty, the joint uncertainty may be sufficiently small relative to the acceptable level of uncertainty defined for the target application decision variables.

4. We can ask several questions concerning the validity of the model, given the experimental observations. First, we can ask whether the experimental observations are likely, given the models for the validation experiments. This first question does not account for the anticipated target application.

5. Secondly, we can ask whether the weighted combination of the measurements is likely (weighted in a fashion to represent the decision variable of the target application), given the suite of models for the validation experiments and the target application. This second approach asks a different question than the first. It does not require that the data from the unit level experiments be likely, only that the weighted measurements be likely. On the other hand, this approach does require that those measurements from the validation experiments that are important to the target application be likely. In fact, we could have the case where the weighted measurements are not likely, but the measurements at strictly the unit level are. For example, we may have very small differences between the predictions and the measurements that are not important to the application, but larger differences in those that are important. Validation at strictly the unit level, using non-application based metrics, will not be able to make this discrimination. The weighted approach presented here can.

6. Lastly, we can ask whether the weighted combination of measurements is within the uncertainty allowed for the application, even though the weighted combination is unlikely relative to the uncertainty in the validation experiments. This approach assumes that there is more allowable uncertainty in the decision variable than in the reconstructed decision variable. This last approach is dangerous. If the weighted measurements are not likely, then the validity of the models are questionable. In this case, we really have to question the validity of the reconstructed decision variable and the validity of any predictions made thereof since they are based on the models. In the present work, we will restrict our attention to the first two approaches.

In the present work, we focus on developing validation metrics, assuming that the models

are correct, or at least approximately correct. If the target application model is incorrect, then we run the risk that the weights chosen for the validation metric at the unit level will be incorrect. However, while the weighting may not be exactly correct, the weights provided by a target application model that roughly approximates the application physics, will provide a much better validation metric than ignoring the target application all together.

2.3.1 Metrics

Consider a set validation measurements $\boldsymbol{\gamma}$, the corresponding covariance matrix cov($\boldsymbol{\gamma}$), the model predictions of the measurements $\mathbf{F}(\boldsymbol{\alpha}, \boldsymbol{\alpha}_v)$, and covariance matrix of the uncertain model parameters $\text{cov}(\boldsymbol{\alpha}_v)$. We are interested in developing a metric for the weighted linear combination of the differences where the weighting is given by **A** (we can simply substitute **P** for **A** in the following derivation for the projection method)**.** The weighted linear combination of differences is given

$$\Delta\mathbf{d} = \mathbf{A}^{\mathrm{T}} [\boldsymbol{\gamma} - \mathbf{F}(\boldsymbol{\alpha}, \boldsymbol{\alpha}_v)] \tag{2.40}$$

The covariance matrix for this linear combination of differences is given by (see Eq. (2.39))

$$\text{cov}(\mathbf{d}) = \mathbf{A}^{\mathrm{T}} \text{cov}(\boldsymbol{\gamma})\mathbf{A} + \mathbf{A}^{\mathrm{T}}\nabla_{\boldsymbol{\alpha}_v}\mathbf{F}(\boldsymbol{\alpha},\boldsymbol{\alpha}_v)\text{cov}(\boldsymbol{\alpha}_v)(\mathbf{A}^{\mathrm{T}}\nabla_{\boldsymbol{\alpha}_v}\mathbf{F}(\boldsymbol{\alpha},\boldsymbol{\alpha}_v))^{\mathrm{T}} \tag{2.41}$$

Note that we have not included the uncertainty for the target application model parameters. We are interested in consistency between the weighted combination of measurements and the validation experiments without adding the uncertainty in the target application model parameters. However, accounting for this uncertainty is straight forward. One just has to restore this term in Eq. (2.41). Collecting terms in **A** in Eq. (2.41) gives

$$\text{cov}(\mathbf{d}) = \mathbf{A}^{\mathrm{T}}\left(\text{cov}(\boldsymbol{\gamma}) + \nabla_{\boldsymbol{\alpha}_v}\mathbf{F}(\boldsymbol{\alpha},\boldsymbol{\alpha}_v)\text{cov}(\boldsymbol{\alpha}_v)(\nabla_{\boldsymbol{\alpha}_v}\mathbf{F}(\boldsymbol{\alpha},\boldsymbol{\alpha}_v))^{\mathrm{T}}\right)\mathbf{A} \tag{2.42}$$

At this point, we ask whether the differences between the weighted combination of measurements and model predictions (i.e., Eq. (2.40)) is significant relevant to the uncertainty in the weighted combination of differences as represented by (2.42). Before we can define significance, we need to know the functional form for the probability distribution for the uncertainty in $\Delta\mathbf{d}$.

2.3.2 Normal Distributions

If the measurements and the model predictions are normally distributed, then a linear combination of these differences (Eq. (2.40)) will be normally distributed with the

covariance defined by Eq. (2.42). For the case of normally distributed differences, we use the following statistic (see Hills and Trucano, 2001):

$$r^2 = \Delta\mathbf{d}^{\mathrm{T}} \, \mathrm{cov}^{+}(\mathbf{d}) \Delta\mathbf{d} \tag{2.43}$$

The + superscript indicates a pseudoinverse. This is presented in Hills and Trucano (2001) for the case of **A** given by the projection matrix **P**. In the case of the projection matrix approach, the rank of the covariance matrix is less than full rank since we remove directions of no importance to the decision variable. For the representative methods, cov(**d**) will also not be of full rank for the case of more measurements than important model parameters, $\boldsymbol{\alpha}$. In this case, cov(**d**) will generally have a rank equal to the number of important parameters for the target application. As such, we take the inverse of cov(**d**) in just that subspace spanned by cov(**d**), and set the remaining contributions to zero. This is accomplished through the use of the pseudoinverse of cov(**d**). Specifically, we use a singular value decomposition and remove those directions for which the singular values are zero (see Hills and Trucano, 2001). Our metric thus only measures differences in the direction of importance to the target application decision variable.

For normally distributed $\Delta\mathbf{d}$, the r^2 statistic is distributed as the $\chi^2(n)$ distribution with n degrees of freedom were n is the rank of the covariance matrix. To differentiate the case for the rank of the covariance matrix that is different from its dimension, we use the symbol n^+ to represent degrees of freedom. Given a value for r^2 from our measurements, we can evaluate the cumulative probability (significance) that a set of measurements give an r^2 value larger than observed, given that the model is valid.

$$\mathrm{P}(\chi^2(n^+) > r^2) \tag{2.44}$$

If the significance is small, we must question the validity of the model or the validity of the probability models used to evaluate this statistic, or both. A small significance suggests that we should first revisit the characterization of the uncertainties in the parameters to ensure that we did not underestimate their uncertainty (a fairly common problem as these estimates are often mistakenly based on the characterization of precision rather than accuracy) and then revisit the suitability of the model and it's boundary and initial conditions.

2.3.3 Mixed Distributions

When the probability density functions for the predictions are non-normal, the difference between prediction and measurement can be difficult to characterize. This is especially true if the computational cost of a function evaluation $\mathbf{F}(\boldsymbol{\alpha}, \boldsymbol{\alpha}_v)$ is large and if the number of predicted measurements is large. An alternative approach is to use Maximum Likelihood to obtain a best estimate of the true model parameters and then evaluate the cumulative probability that the probability density of the estimated parameters are less than the values estimated. This approach was developed in Hills and Trucano (2002) and

was shown to give the same significance as the approach outlined under Section 2.3.2 for normally distributed parameters and measurements, with models locally linear in the parameters.

The Maximum Likelihood approach used by Hills and Trucano (2002) evaluates the model parameters $\boldsymbol{\alpha}_v$ that maximize the joint probability density

$$\text{PDF}(\boldsymbol{\gamma}, \langle\boldsymbol{\gamma}\rangle)\ \text{PDF}(\boldsymbol{\alpha}_v, \langle\boldsymbol{\alpha}_v\rangle) \tag{2.45}$$

subject to the constraint

$$\langle\boldsymbol{\gamma}\rangle = \mathbf{F}(\boldsymbol{\alpha}, \boldsymbol{\alpha}_v) \tag{2.46}$$

The $\langle\rangle$ represent expected value. We can use other measures of central tendency such as median or mode. Note that we are assuming a valid model will provide predictions, when evaluated at the true value of the model parameters, that agree with this measure of central tendency of the measurements (see Hills and Trucano, 2002). Here we modify the approach and incorporate the weighted measurements. While we show the development for the matrix **A**, the same development applies to the matrix **P**. We wish to maximize

$$\text{PDF}(\mathbf{A}\boldsymbol{\gamma}, \langle\mathbf{A}\boldsymbol{\gamma}\rangle)\ \text{PDF}(\boldsymbol{\alpha}_v, \langle\boldsymbol{\alpha}_v\rangle) \tag{2.47}$$

subject to the constraint given by Eq. (2.46). The known parameters in Eq. (2.47) are $\langle\boldsymbol{\alpha}_v\rangle$ from our knowledge of the distribution of the uncertain model parameters, and $\mathbf{A}\boldsymbol{\gamma}$ which follows directly from our measurements and weighting matrix. A function evaluation routine must be provided to the optimization routine to evaluate the objective function given a guess for the parameter vector $\boldsymbol{\alpha}_v$. The function routine does the following:

1. Given a guess for the parameter vector $\boldsymbol{\alpha}_v$, and the appropriate values for $\boldsymbol{\alpha}$ (note that we are assuming the uncertain parameters are $\boldsymbol{\alpha}_v$ and that $\boldsymbol{\alpha}$ is known exactly), we evaluate $\langle\boldsymbol{\gamma}\rangle$ from our model, Eq. (2.46).

2. Given $\langle\boldsymbol{\gamma}\rangle$, our observed measurements (containing error) $\boldsymbol{\gamma}$, and our a-priori knowledge of $\langle\boldsymbol{\alpha}_v\rangle$, we can evaluate the negative of the corresponding joint probability density from Eq. (2.47). We return the negative since our optimization routine minimizes, when, in fact, we wish to maximize.

3. The previous steps are repeated for different iterations on the parameter values $\boldsymbol{\alpha}_v$ until the $\min(-\text{PDF}(\mathbf{A}\boldsymbol{\gamma}, \langle\mathbf{A}\boldsymbol{\gamma}\rangle)\ \text{PDF}(\boldsymbol{\alpha}_v, \langle\boldsymbol{\alpha}_v\rangle))$ is found.

Once we have our best estimate for $\boldsymbol{\alpha}_v$, we use this estimate to define a validation metric that is appropriate for our target application. If our model is valid, our uncertainty will be due only to uncertainty in the model parameters and the experimental measurements. The PDF for our uncertainty is defined by (2.47) at our maximum likelihood estimate for $\boldsymbol{\alpha}_v$.

We would like to evaluate the cumulative probability of obtaining this probability density, or smaller, to evaluate the significance of the observed measurements, given that the model is valid. Here we use a Monte Carlo analysis (Hills and Trucano, 1999).

The Monte Carlo analysis used here is fairly straightforward and only requires one model evaluation.

1. Evaluate the $<\gamma>$ from Eq. (2.46) using the α_v obtained from the optimization procedure.

2. Generate a γ from the PDF(γ, $<\gamma>$), evaluate Eq. (2.47) using the estimated α_v.

3. Repeat step 2 multiple times and count the number of times the value for the joint PDF evaluated in step 2 is less than the PDF obtained from the optimization procedure. If this process is repeated a sufficient number of times, the % of times the joint PDF is smaller than that estimated from the optimization process approximates the cumulative probability (i.e., significance) that a valid model would have measurements this far or further from those observed.

As was shown in Hills and Trucano (2002), this Maximum Likelihood approach and that presented in the previous section provides the same cumulative probability for normally distributed measurements and validation model parameters, for a model that is locally linear in the parameters.

3.0 Example Applications

3.1 Introduction

In this chapter, we work through a series of examples to demonstrate the use of the methodology presented in the previous chapter. These are presented in the order of simple to complex and address issues of coverage of the target application by the validation experiments, sensitivity of the reconstructed decision variable to the uncertainties in the validation experiments, and the construction of application-based validation metrics.

3.2 Simple Heat Conduction: 2 Measurements

Consider the one-dimensional thermal heat conduction problem illustrated in Figure 3.1.

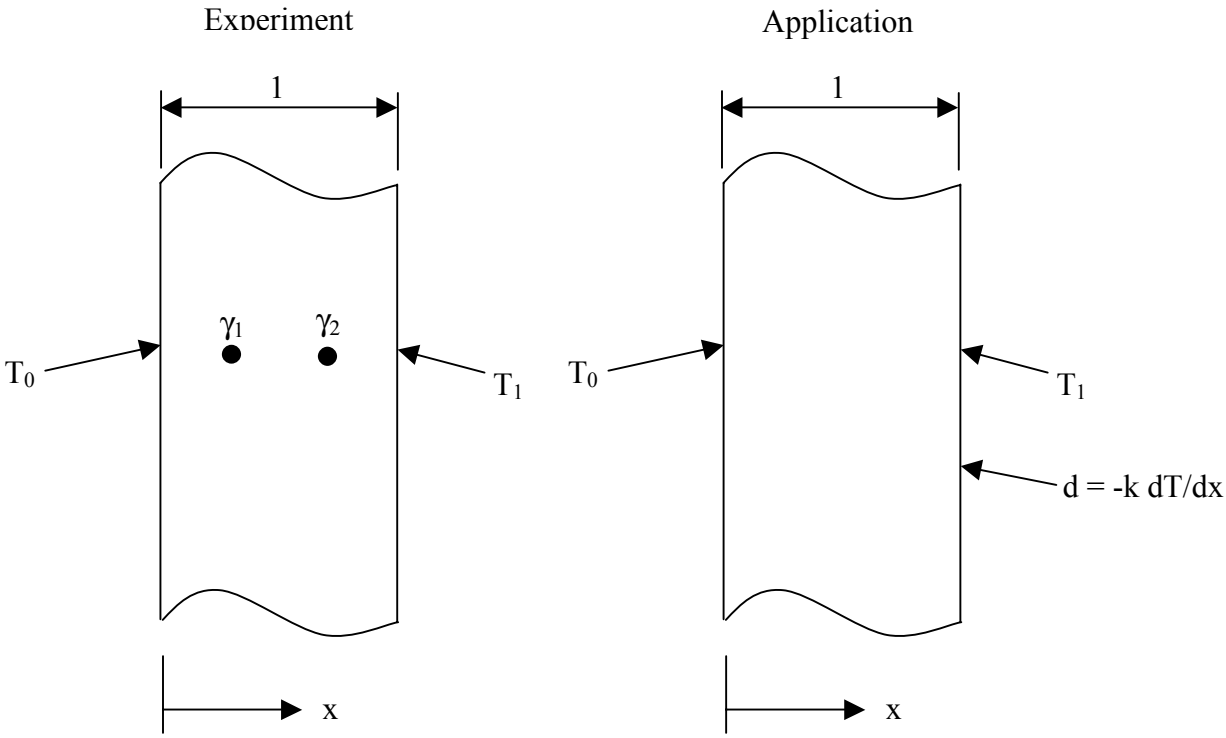

Figure 3.1: Example 1: Heat Conduction

We assume the validation experiment and the target application have the same geometry

and materials and that there are no uncertainties in the geometry or in the material properties. For the validation experiment, we assume that we have internal temperature measurements and no measure of flux on the surface. In contrast, we take our decision variable to be heat flux measured on the surface. We assume the uncertainty in the measurements have a uniform standard deviation σ_m and that the measurement uncertainties at each measurement location are uncorrelated.

We will use the methodology developed in the previous chapter to answer the following questions:

1. Are the measurements taken from the validation experiments adequate to represent the decision variable of the target application?

2. If the answer to item 1 is in the affirmative, how should we weight the measurements to best represent the target application?

3. What is the sensitivity of this representation to the measurement uncertainty?

4. Is the uncertainty in the measurements sufficiently small to adequately represent the target application?

We begin by presenting the mathematical formulation for the problem. Assume that our models for the validation experiment and the target application are given by

Experiment:	Application:	
$\frac{d^2T}{dx^2} = 0$	$\frac{d^2T}{dx^2} = 0$	(3.1)
$T(0) = T_0 = \alpha_1$	$T(0) = T_0 = \alpha_1$	(3.2a,b)
$T(1) = T_1 = \alpha_2$	$T(1) = T_1 = \alpha_2$	(3.2c,d)
$\gamma_1 = T(0.25)$	$d = -k\, dT(1)/dx$	(3.3a,b)
$\gamma_2 = T(0.75)$		(3.3c)

The uncertainty in the measurements can be written in terms of the covariance matrix of $\boldsymbol{\gamma}$.

$$\mathrm{cov}(\boldsymbol{\gamma}) = \sigma_m^{\,2} \begin{bmatrix} 1 & 0 \\ 0 & 1 \end{bmatrix} = \sigma_m^{\,2}\, \mathbf{I} \tag{3.4}$$

where $\mathbf{I}$ is the identity matrix. Since we have simple models, we can illustrate this

example using closed form solutions rather than numerical solutions. The solutions are given by

Experiment:	Application:	
$T = \alpha_1(1-x) + \alpha_2 x$	$T = \alpha_1(1-x) + \alpha_2 x$	(3.5a,b)

The measurements and decision variables are thus given by

Experiment:	Application:	
$\gamma_1 = 0.75\alpha_1 + 0.25\alpha_2$	$d = k(\alpha_1 - \alpha_2)$	(3.6a,b)
$\gamma_2 = 0.25\alpha_1 + 0.75\alpha_2$		(3.6c)

Performing a first order sensitivity analysis gives (see Eqs. (2.3) and (2.4))

Experiment:	Application:	
$\nabla_{\boldsymbol{\alpha}}\mathbf{F} = \begin{bmatrix} 0.75 & 0.25 \\ 0.25 & 0.75 \end{bmatrix}$	$\nabla_{\boldsymbol{\alpha}}\mathbf{G} = \begin{bmatrix} k & -k \end{bmatrix}$	(3.7a,b)

so

$$\begin{bmatrix} 0.75 & 0.25 \\ 0.25 & 0.75 \end{bmatrix}\mathbf{a} = \begin{bmatrix} k \\ -k \end{bmatrix} \tag{3.8}$$

Note that the two columns of the matrix are independent. We can thus represent any vector on the right hand side of Eq. (3.8) as a linear combination of the columns in the matrix. Thus, we can write the sensitivity of the target application to the important model parameters $\boldsymbol{\alpha}$ in terms of the sensitivities of our validation experiments to these parameters.

Solving for **a** gives

$$\mathbf{a} = \begin{bmatrix} 2k \\ -2k \end{bmatrix} \tag{3.9}$$

Using these results in Eq. (2.12) and (3.3) gives

$$\Delta d = \mathbf{a}^{\mathrm{T}}\Delta\boldsymbol{\gamma} = -k\frac{\Delta\gamma_2 - \Delta\gamma_1}{0.5} = -k\frac{\Delta T(0.75) - \Delta T(0.25)}{0.5} \tag{3.10}$$

Note that Eq. (3.10) is simply the first order finite difference approximation to the flux. In other words, this methodology does, in fact, tell us how to weight the measurements (strictly speaking, differences in the measurements), to best represent the decision variable for the target variable. Given the weighting **a**, we can evaluate the corresponding uncertainty in the decision variable d. The covariance matrix of Δd is given by (see Eq. (2.16))

$$\text{cov}(d) = \sigma_d^2 = \mathbf{a}^T \text{cov}(\boldsymbol{\gamma})\, \mathbf{a} \tag{3.11}$$

Using Eq. (3.9) gives

$$\sigma_d^2 = \sigma_m^2\, \mathbf{a}^T \mathbf{I}\, \mathbf{a} = 8\, \sigma_m^2\, k^2 \tag{3.12}$$

Note that the variance in the approximation to changes in the target variable is 8 times the conductivity-squared times the variance in the measurement variables.

What does all this mean? First, a first-order model for the sensitivity of the target decision variable to the model parameters can be represented by a linear combination of first order models for the predicted validation measurements. A weighting of the validation experiment measurements can be defined to represent the target application. In other words, the measurements can be weighted to represent the sensitivity of the target decision variable to the model parameters. Secondly, the variance in the reconstructed decision variable is $8k^2$ times the variance of the measurements. If the acceptable level of uncertainty in the decision variable for the actual target application is, say $2k^2$; then the validation experiment must be designed so that the corresponding variance in the measurements is less than 0.25, i.e.;

$$8\, \sigma_m^2\, k^2 < 2\, k^2 \Rightarrow \sigma_m^2 < 0.25 \tag{3.13}$$

Note that at the $\sigma_m^2 = 0.25$ level, the uncertainty in the validation measurements equals the uncertainty allowed in the target application. In fact, we should require that the uncertainty in the validation measurements be much less since there will be other sources of uncertainty in the target application, such as larger levels of uncertainty in the model parameters (we can almost always control validation experiments at a finer level then we can target applications). We will show the effect of uncertainty in the model parameters in a later section.

3.3 Simple Heat Conduction: 2 Validation Experiments

Consider the one-dimensional thermal heat conduction problem illustrated in Figure 3.2. In this example, we again assume that the validation experiments and the target application have the same geometry and materials and that there are no uncertainties in the geometry or materials. For validation experiment 1, we assume that we have internal

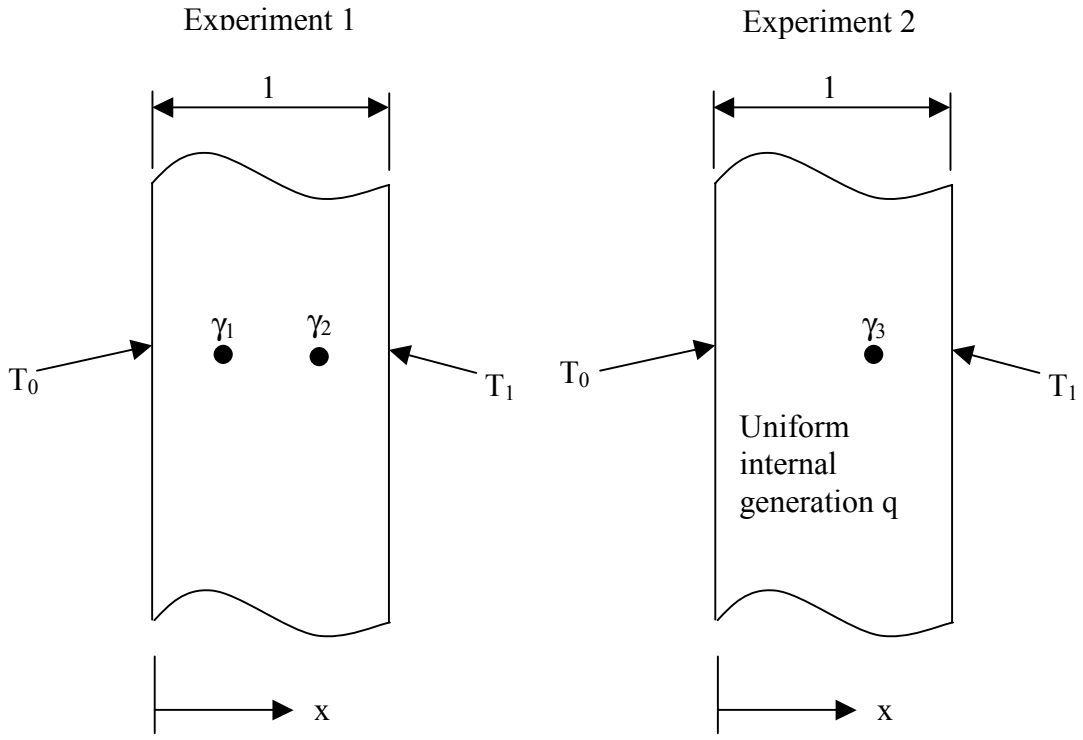

Figure 3.2: Example 2: Heat Conduction Validation Experiments

temperature measurements and no measure of flux on the surface, nor internal generation. We design validation experiment 2 to have uniform internal generation with a single temperature measurement made at $x=x_v$ in the interior. As in the previous case, our decision variable is the flux at the x=1 surface. Our target application is given in Figure 3.3. Note that the decision variable is again flux at x=1. The target application contains uniform internal generation.

We assume that the important model parameters are the boundary conditions at x=0 and x=1, and the internal generation q. We also assume that the covariance matrix for the validation measurements is given by

$$\mathrm{cov}(\boldsymbol{\gamma}) = \sigma_m^{\,2} \begin{bmatrix} 1 & 0 & 0 \\ 0 & 1 & 0 \\ 0 & 0 & 1 \end{bmatrix} = \sigma_m^{\,2}\,\mathbf{I} \tag{3.14}$$

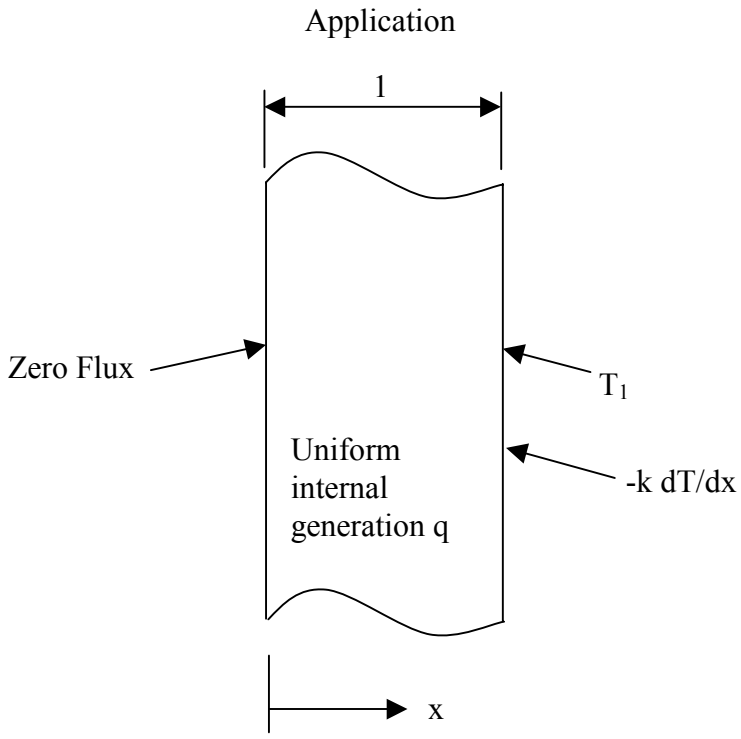

Figure 3.3: Example 2: Target Application

Our models for the two validation experiments are

Experiment 1:	Experiment 2:	
$\frac{d^2T}{dx^2} = 0$	$\frac{d^2T}{dx^2} = q = \alpha_3$	(3.15a,b)
$T(0) = T_0 = \alpha_1$	$T(0) = T_0 = \alpha_1$	(3.16a,b)
$T(1) = T_1 = \alpha_2$	$T(1) = T_1 = \alpha_2$	(3.16c,d)
$\gamma_1 = T(0.25)$	$\gamma_3 = T(x_v)$	(3.17a,b)
$\gamma_2 = T(0.75)$		(3.17c)

The model for our target application is

$$\frac{\mathrm{d}^2 T}{\mathrm{d}x^2} = q = \alpha_3 \tag{3.18}$$

$$dT(0)/dx = 0 \tag{3.19a}$$
$$T(1) = T_1 = \alpha_2 \tag{3.19b}$$

$$d = -k\, dT(1)/dx \tag{3.20}$$

Since we have simple models, we can illustrate this example using closed form solutions rather than numerical solutions. The solutions are given by

Experiment 1: Experiment 2:

$$T = \alpha_1(1-x) + \alpha_2 x \qquad T = \alpha_1(1-x) + \alpha_2 x + \frac{\alpha_3}{2}(x^2 - x) \tag{3.21a,b}$$

The measurements are thus given by

Experiment 1: Experiment 2:

$$\gamma_1 = 0.75\alpha_1 + 0.25\alpha_2 \qquad \gamma_3 = \alpha_1(1-x_v) + \alpha_2 x_v + \frac{\alpha_3}{2}(x_v^2 - x_v) \tag{3.22a,b}$$
$$\gamma_2 = 0.25\alpha_1 + 0.75\alpha_2 \tag{3.23}$$

The solution for our target application is

$$T = \alpha_2 + \frac{\alpha_3}{2}(x^2 - 1) \tag{3.24}$$

The decision variable is

$$d = -k\alpha_3 \tag{3.25}$$

Performing a first order sensitivity analysis gives (see Eqs. (2.3), (2.4), (3.24), (3.25))

Experiment: Application:

$$\nabla_{\boldsymbol{\alpha}}\mathbf{F} = \begin{bmatrix} 0.75 & 0.25 & 0 \\ 0.25 & 0.75 & 0 \\ 1-x_v & x_v & \left(x_v^2 - x_v\right)/2 \end{bmatrix} \qquad \nabla_{\boldsymbol{\alpha}}\mathbf{G} = \begin{bmatrix} 0 & 0 & -k \end{bmatrix} \tag{3.26a,b}$$

We will now consider three cases. These are 1) the use of experiment 1 only, 2) the use of experiment 2 only, and 3) the use of both experiments.

3.3.1 Case 1: Experiment 1 Only

In this case, we use only the first two rows of Eq. (3.26a) corresponding to Experiment 1.

$$\nabla_{\alpha}\mathbf{F} = \begin{bmatrix} 0.75 & 0.25 & 0 \\ 0.25 & 0.75 & 0 \end{bmatrix} \qquad \nabla_{\alpha}\mathbf{G} = \begin{bmatrix} 0 & 0 & -k \end{bmatrix} \tag{3.27a,b}$$

so

$$\begin{bmatrix} 0.75 & 0.25 \\ 0.25 & 0.75 \\ 0 & 0 \end{bmatrix} \mathbf{a} = \begin{bmatrix} 0 \\ 0 \\ -k \end{bmatrix} \tag{3.28}$$

Note that while the two columns of the matrix are independent, they cannot represent the right hand side. No linear combination of these columns can represent the right hand side for a non-zero k. In the context of the present method, the first validation experiment, by itself, cannot represent the target application. This is not surprising since we considered internal generation as an important parameter which is not present in the first validation experiment. Because a solution to Eq. (3.28) does not exist, we cannot pursue this problem further without additional experiments.

3.3.2 Case 2: Experiment 2 Only

In this case, we use only the last row of Eq. (3.26a) corresponding to Experiment 2.

$$\nabla_{\alpha}\mathbf{F} = \begin{bmatrix} 1 - x_v & x_v & \left(x_v{}^2 - x_v\right)/2 \end{bmatrix} \qquad \nabla_{\alpha}\mathbf{G} = \begin{bmatrix} 0 & 0 & -k \end{bmatrix} \tag{3.29a,b}$$

so

$$\begin{bmatrix} 1 - x_v \\ x_v \\ \dfrac{x_v{}^2 - x_v}{2} \end{bmatrix} a = \begin{bmatrix} 0 \\ 0 \\ -k \end{bmatrix} \tag{3.30}$$

Note that there is no x_v that gives zeros in the first two elements of the left hand side. Thus, we cannot find an a that satisfies Eq. (3.30). In the context of the present method,

the second validation experiment by itself, cannot represent the target application. This is a bit more surprising since the second application contains the same physics as the target application. However, we cannot reconstruct the decision variable, heat flux, without the additional internal measurements. This suggests that we may need to use both validation experiments to resolve the target application decision variable.

3.3.3 Case 3: Experiments 1 and 2

In this case, we use all of Eq. (3.26a)

Experiment: Application:

$$\nabla_{\alpha}\mathbf{F}=\begin{bmatrix} 0.75 & 0.25 & 0 \\ 0.25 & 0.75 & 0 \\ 1-x_v & x_v & \left(x_v{}^2-x_v\right)/2 \end{bmatrix} \qquad \nabla_{\alpha}\mathbf{G}=\begin{bmatrix} 0 & 0 & -k \end{bmatrix} \tag{3.31a,b}$$

so

$$\begin{bmatrix} 0.75 & 0.25 & 1-x_v \\ 0.25 & 0.75 & x_v \\ 0 & 0 & \dfrac{\left(x_v{}^2-x_v\right)}{2} \end{bmatrix}\mathbf{a}=\begin{bmatrix} 0 \\ 0 \\ -k \end{bmatrix} \tag{3.32}$$

Do the columns of the matrix span the right hand side of Eq. (3.32)? The answer to this question depends on the value for x_v. For example, if we take $x_v = 0$, Eq. (3.32) gives

$$\begin{bmatrix} 0.75 & 0.25 & 1 \\ 0.25 & 0.75 & 0 \\ 0 & 0 & 0 \end{bmatrix}\mathbf{a}=\begin{bmatrix} 0 \\ 0 \\ -k \end{bmatrix} \tag{3.33}$$

Clearly, no linear combination of the columns of the coefficient matrix can reproduce the $-k$ term in the right hand side. If $x_v = 1$, then all the elements in the last row of the coefficient matrix are also zero, leading to the same results. Taking measurements on the boundaries of the second validation experiment does not help us resolve the effect of internal generation in the target application. In contrast, there is a unique solution to Eq. (3.33) for interior x_v. For example, taking the measurement from the center of the conducting slab, $x_v = 0.5$, results in

$$\begin{bmatrix} 0.75 & 0.25 & 0.5 \\ 0.25 & 0.75 & 0.5 \\ 0 & 0 & -0.125 \end{bmatrix} \mathbf{a} = \begin{bmatrix} 0 \\ 0 \\ -k \end{bmatrix} \tag{3.34}$$

which does have a unique solution. Thus this set of experiments can represent the sensitivities of the target application to the important model parameters. Solving for **a** gives

$$\mathbf{a} = k \begin{bmatrix} -4 \\ -4 \\ 8 \end{bmatrix} \tag{3.35}$$

Using this in Eq. (2.16) gives

$$\sigma_d^2 = \sigma_m^2 \, \mathbf{a}^T \mathbf{I} \, \mathbf{a} = 96 \, \sigma_m^2 \, k^2 \tag{3.36}$$

While these measurements can be weighted to represent the target application, we see that our estimate of the corresponding decision variable is very sensitive to the measurement error. In other words, while the suite of experiments are appropriate for the target application, the experiments were selected in a fashion that the resulting representation of the decision variable is very sensitive to small errors in the measurements. Can we improve this by taking the internal temperature measurement from experiment 2 at some other location x_v? The x_v that minimizes Eq. (2.16), given Eq. (3.32), can be shown to be $x_v = 0.5$. So x_v is already optimum. However, we may be able to reduce the sensitivity to the measurements noise by using additional measurements.

Consider two measurements taken in experiment 2 at $x = 0.5 - \delta$ and $x = 0.5 + \delta$.

In this case, the Eq. (3.32) becomes

$$\begin{bmatrix} 0.75 & 0.25 & 0.5+\delta & 0.5-\delta \\ 0.25 & 0.75 & 0.5-\delta & 0.5+\delta \\ 0 & 0 & \dfrac{(0.5-\delta)^2 + \delta - 0.5}{2} & \dfrac{(0.5+\delta)^2 - \delta - 0.5}{2} \end{bmatrix} \mathbf{a} = \begin{bmatrix} 0 \\ 0 \\ -k \end{bmatrix} \tag{3.37}$$

Note that since we have 4 measurements, but are only attempting to represent the sensitivity of the system to 3 parameters, the system has one free variable. There are an infinity of solutions for $\delta \neq \pm 0.5$ (i.e., the two measurements in the interior of the conducting solid). We choose the solution that minimizes the following

$$\sigma_d^2 = \sigma_m^2 \, \mathbf{a}^T \mathbf{I} \, \mathbf{a} \tag{3.38}$$

subject to the constraints given by Eq. (3.37) using the Lagrange multipliers as discussed in the previous chapter. For example, if we take $\delta = .25$, we find

$$\mathbf{a} = k\begin{bmatrix} -5.333 \\ -5.333 \\ 5.333 \\ 5.333 \end{bmatrix} \tag{3.39}$$

Using Eq. (2.16) gives

$$\sigma_d^2 = \sigma_m^2\, \mathbf{a}^T\, \mathbf{I}\, \mathbf{a} = 113.8\, \sigma_m^2\, k^2 \tag{3.40}$$

Searching through all possible δ to find the one that minimizes Eq. (3.38) gives $\delta = 0$. This is equivalent to taking two independent measurements at the same location, the center of the slab. This can be accomplished by installing two thermal couples along the centerline. The corresponding weighting of the 4 measurements is

$$\mathbf{a} = k\begin{bmatrix} -4 \\ -4 \\ 4 \\ 4 \end{bmatrix} \tag{3.41}$$

with

$$\sigma_d^2 = \sigma_m^2\, \mathbf{a}^T\, \mathbf{I}\, \mathbf{a} = 64\, \sigma_m^2\, k^2 \tag{3.42}$$

We see that the use of two measurements in experiment 2 does improve the ability to resolve the decision variable somewhat, but the weighting of the measurements to represent the decision variable is still very sensitive to the measurements uncertainty.

This last example shows the power of the present approach. The approach not only shows how to weight the measurements to resolve the first order sensitivity of the decision variables for the target application to the measurements, but also relates uncertainty in the validation measurements to the corresponding uncertainty in the reconstruction of the decision variable. Comparing Eqs. (3.12) to (3.42), we see that the sensitivity to measurement error in the internal temperature measurements is much greater for our target application with internal generation than for that without internal generation.

In the following section, we introduce a more complex example that includes the effect of uncertainty in the unit and system level models to uncertainty in the model parameters. This has the effect of increasing the overall uncertainty in the reconstructed decision variable.

3.4 Transient Heat Conduction with Parameter Uncertainty

We now look at a transient heat conduction problem in the presence of model parameter uncertainty. Consider the following models for the unit level experiments and application:

Experiment:	**Application:**	
$\frac{\partial T}{\partial t} = \frac{k}{\rho C_p}\frac{\partial^2 T}{\partial x^2}$	$\frac{\partial T}{\partial t} = \frac{k}{\rho C_p}\frac{\partial^2 T}{\partial x^2}$	(3.43a,b)
$T(x,0)=0$	$T(x,0)=0$	(3.44a,b)
$T(0,t) = T_0$	$T(0,t) = T_0$	(3.44c,d)
$T(1,t) = T_1$	$T(1,t) = T_1$	(3.44,e,f))
$\gamma_1 = T(0.25,t_j), j=1,n$	$d = -k\, d\mathrm{T}(1,t_a)/d\mathrm{x}$	(3.45a,b)
$\gamma_2 = T(0.75,t_j), j=1,n$		(3.45c)

Note that the above is the transient version of the first example problem presented previously. This problem adds considerable complication in that we have measurements taken at various spatial and temporal locations and our decision variable is sampled at discrete times. We take the following variables as important and/or uncertain to the model.

Experiment:	**Application:**
Important: T_0, T_1, k, ρC_p	Important: T_0, T_1, k, ρC_p
Uncertain: k	Uncertain: T_0, T_1, k, ρC_p

Note that we are assuming that we can measure the boundary temperatures accurately for the validation experiment, but that we will have uncertainty in the target application boundary temperatures simply because we cannot run the application *a-priori*. Also, note that we have uncertainty in the thermal conductivity in both cases, but also have uncertainty in the heat capacity for the decision variable. This example was chosen to illustrate that we can have different parameters with different uncertainties for the validation experiments and the target application. The parameters important to both models are

$$\alpha_1 = T_0,\ \alpha_2 = T_1,\ \alpha_3 = k,\ \alpha_4 = \rho C_p \tag{3.46}$$

The unit and system level uncertain parameters are

$$\alpha_{v1} = k\ ,\ \alpha_{a1} = T_1,\ \alpha_{a2} = T_2,\ \alpha_{a3} = k,\ \alpha_{a4} = \rho C_p \tag{3.47}$$

Due to the simple form of our models, we use a closed form (Carslaw and Jaeger, 1978) solution to the Eqs. (3.43) and (3.44).

$$T(x,t) = T_1(1-x) + T_2\, x + \sum_{n=1}^{\infty} A_n \exp\left(-\frac{k}{\rho C_p}(n\pi)^2 t\right)\sin(n\pi x) \tag{3.48}$$

where

$$A_n = -\frac{2}{n\pi}\left[T_1 - T_2(-1)^n\right] \tag{3.49}$$

Our decision variable is given by (see Eq. (3.45b))

$$d(t) = -k\left(T_2 - T_1 + \sum_{n=1}^{\infty} A_n\, n\pi \exp\left(-\frac{k}{\rho C_p}(n\pi)^2 t\right)\cos(n\pi x)\right) \tag{3.50}$$

Let's assume that the mean model parameters and their corresponding uncertainties are given by the values shown in Table 3.1. We also show the uncertainty in the measurements.

Table 3.1: Model Parameters and Temperature Measurements

Parameter	Mean Value	Standard Deviation
Validation Experiment		
k	1.0	0.05
γ		0.25
Application		
T_1	10.0	2.0
T_2	20.0	2.0
k	1.0	0.1
ρC_p	1.0	0.1

For much of this analysis, we do not need to assume a functional form for the probability density functions. However, the statistical inference for model validity will require that we make additional assumptions concerning the underlying distributions. At that time, we will assume that the uncertainties for these parameters can all be modeled by independent normal distributions. Note that we show more uncertainty in the thermal conductivity for the target application than we do for the unit level validation experiments. We expect our validation experiments to be better controlled than our target applications. Rather than evaluate the sensitivity derivatives by differentiating (3.48) and (3.50) directly, we will

use finite differences to estimate these derivations. This is simply a convenience, but also is typical of the method used to evaluate more complex models that must be solved numerically. The times at which the measurements are taken are given in Table 3.2. We also show predicted measurements using the mean parameter values listed in Table 3.1. Simulated experimental measurements are also provided. These measurements were generated using the following procedure:

1. Randomly generate a set of validation model parameters using the probability distribution for the parameters. For this case, we have one model parameter, *k*, with the statistics given in Table 3.1. We randomly generate this parameter because we are uncertain as to what the parameter should be for the actual validation experiment.

2. Given the set of parameters, use the model to generate a set of predicted measurements.

3. Add random noise to the predicted measurements to represent the measurement noise. In this case, we assumed a normal distribution for each of the measurements with the statistics given in Table 3.1.

This procedure generates a set of measurements that we may obtain if the model were valid. To make the analysis more interesting, we repeated the above procedure multiple times until a significant, but low probability, set of measurements was obtained. We did this to demonstrate the methodology when the measurements were near the region of non-acceptance for a model. The resulting measurements are shown in the last column of Table 3.2.

Table 3.2: Temperature Predictions and Measurements

Time	x	Tpred	Tmeas
0.10	0.25	7.53	8.30
0.25	0.25	11.35	12.00
0.50	0.25	12.40	12.38
0.75	0.25	12.49	12.85
1.00	0.25	12.50	12.69
0.10	0.75	12.40	12.68
0.25	0.75	16.35	16.24
0.50	0.75	17.40	17.56
0.75	0.75	17.49	17.70
1.00	0.75	17.50	17.00

The sensitivity coefficients for these measurement times and locations are given in Table 3.3. These were obtained using forward first order finite differences with a step size of 0.01 times the mean value for that parameter.

Table 3.3: Sensitivity Coefficients for Validation Model Parameters

Time	x	$\frac{\partial \mathbf{F}}{\partial T_1}$	$\frac{\partial \mathbf{F}}{\partial T_2}$	$\frac{\partial \mathbf{F}}{\partial k}$	$\frac{\partial \mathbf{F}}{\partial \rho C_p}$
0.10	0.25	0.5761	0.08834	4.711	-4.704
0.25	0.25	0.7118	0.2118	2.710	-2.831
0.50	0.25	0.7468	0.2468	0.4677	-0.4863
0.75	0.25	0.7497	0.2497	0.05877	-0.06263
1.00	0.25	0.7410	0.2500	0.006565	-0.007170
0.10	0.75	0.08834	0.5766	5.186	-5.193
0.25	0.75	0.2118	0.7118	2.793	-2.834
0.50	0.75	0.2468	0.7468	0.4677	-0.4863
0.75	0.75	0.2497	0.7497	0.05877	-0.06263
1.00	0.75	0.2500	0.7500	0.006565	-0.007170

The sensitivity coefficients for the target application are listed in Table 3.4 using the same finite difference technique as was used for Table. 3.3

Table 3.4: Sensitivity Coefficients for Target Application Model

Time	$\frac{\partial \mathbf{G}}{\partial T_1}$	$\frac{\partial \mathbf{G}}{\partial T_2}$	$\frac{\partial \mathbf{G}}{\partial k}$	$\frac{\partial \mathbf{G}}{\partial \rho C_p}$
0.125	0.4319	-1.597	-5.270	-22.20
0.250	0.8305	-1.170	-2.554	-12.59
0.375	0.9506	-1.049	-6.044	-5.531
0.500	0.9856	-1.014	-8.333	-2.161
0.625	0.9958	-1.004	-9.366	-0.7914
0.750	0.9988	-1.001	-9.773	-0.2783
0.875	0.9996	-1.000	-9.922	-0.09513
1.000	0.9999	-1.000	-9.974	-0.03186
10.00	1.0000	-1.000	-10.00	0.000

Given these sensitivities, we use Eq. (2.26) to evaluate the weighting matrix **A**.

$$\mathbf{A} = \left(\text{cov}(\boldsymbol{\gamma})\right)^{-1}\left(\nabla_{\boldsymbol{\alpha}}\mathbf{F}(\boldsymbol{\alpha})\right)\left(\left(\nabla_{\boldsymbol{\alpha}}\mathbf{F}(\boldsymbol{\alpha})\right)^{\mathrm{T}}\left(\text{cov}(\boldsymbol{\gamma})\right)^{-1}\left(\nabla_{\boldsymbol{\alpha}}\mathbf{F}(\boldsymbol{\alpha})\right)\right)^{-1}\left(\nabla_{\boldsymbol{\alpha}}\mathbf{G}(\boldsymbol{\alpha})\right)^{\mathrm{T}} \tag{2.26}$$

The standard deviation of the decision variable as a function of time for the reconstructed decision variables can now be evaluated from Eq. (2.39).

$$\begin{aligned}\text{cov}(\mathbf{d}) = \mathbf{A}^{\mathrm{T}}\,\text{cov}(\boldsymbol{\gamma})\mathbf{A} + \mathbf{A}^{\mathrm{T}}\nabla_{\boldsymbol{\alpha}_v}\mathbf{F}(\boldsymbol{\alpha},\boldsymbol{\alpha}_v)\,\text{cov}(\boldsymbol{\alpha}_v)(\mathbf{A}^{\mathrm{T}}\nabla_{\boldsymbol{\alpha}_v}\mathbf{F}(\boldsymbol{\alpha},\boldsymbol{\alpha}_v))^{\mathrm{T}} \\ + \nabla_{\boldsymbol{\alpha}_a}\mathbf{G}(\boldsymbol{\alpha},\boldsymbol{\alpha}_a)\,\text{cov}(\boldsymbol{\alpha}_a)(\nabla_{\boldsymbol{\alpha}_a}\mathbf{G}(\boldsymbol{\alpha},\boldsymbol{\alpha}_a))^{\mathrm{T}}\end{aligned} \tag{2.39}$$

The standard deviation for each measurement time is given by the square root of the diagonal elements in the matrices that make up Eq. (2.39). The results are given in Table 3.5. The second column shows the contribution due to measurement uncertainty (first term on RHS of Eq. (2.39)), the third column is the contribution due to parameter uncertainty in the unit level model (second term on the RHS of Eq. (2.39)), the fourth column is the contribution due to uncertainty in the target application model (last term on RHS), and the last column gives the total uncertainty.

Table 3.5: Distribution of Uncertainty in Decision Variable

Time	$\sigma_{d\text{-meas}}$	$\sigma_{d\text{-v}}$	$\sigma_{d\text{-a}}$	σ_{d}
0.125	141.6	0.263	4.02	141.7
0.250	78.1	0.128	3.14	78.1
0.375	59.7	0.30	2.95	59.8
0.500	54.1	0.42	2.96	54.2
0.625	52.4	0.47	2.99	52.5
0.750	51.9	0.49	2.99	52.0
0.875	51.7	0.50	3.00	51.8
1.000	51.6	0.50	3.00	51.7
10.00	51.6	0.50	3.00	51.7

Note that the uncertainty in the reconstructed decision variable is greatest at early time and decreases toward steady state. The sensitivity to noise in the measurements decreases as one approaches steady state. We expect this since the surface flux at latter times is dependent on internal temperatures at earlier times. At latter times, we effectively have more internal measurements and we gain the advantage of a reduced standard deviation in the reconstructed decision variable due to this additional data. The sensitivity due to the uncertain model parameter, thermal conductivity, also increases as we approach steady state. At zero time, we assumed no uncertainty in the initial conditions. As we move away from time zero, the uncertainty in the reconstructed flux increases because of our uncertainty in thermal conductivity. Unlike the effect of measurement uncertainty, the effect of uncertainty in the predicted measurements due to uncertainty in thermal conductivity is fully correlated. There is no advantage gained by additional

measurements. In contrast, the uncertainty in the reconstructed decision variable due to uncertainty in the target application uncertainty variables is larger simply because these variables include uncertainties in thermal conductivity, thermal diffusivity, and the temperature at both boundaries. However, the last column of Table 3.5 clearly indicates that the total uncertainty is most dependent on the uncertainty in the temperature measurements from the validation experiment.

There are several conclusions that we can state for this example problem. First, the transient validation experiments do cover the target application decision variable, even though we take measurements at different times, and the decision variable is different than the variables measured for the validation experiments. We know this because we did not obtain a singular matrix during the analysis (or unreasonably high covariances for the decision variable). The results of Table 3.5 indicate that the sensitivity of the reconstructed decision variable decreases as we approach steady state. However, the decision variable is still excessively sensitive to measurement noise in the validation experiments. An additional example addressing this issue will be presented in Sections 3.6 and 3.7.

The examples presented so far address coverage of the target application decision variable by the validation experiments. We now address the use of these results to develop a validation metric.

3.5 Transient Heat Conduction with Parameter Uncertainty: Validation

In this example, we use the transient example discussed in the previous section. We begin by applying the metric developed in Hills and Trucano (2001) for the validation data that does not account for the target application. For normally distributed model parameters and the sensitivity analysis presented above, this metric is

$$r^2 = (\mathbf{F}(\boldsymbol{\alpha}, <\boldsymbol{\alpha}_v>) - \boldsymbol{\gamma})^{\mathrm{T}} \operatorname{cov}(\mathbf{F} - \boldsymbol{\gamma})(\mathbf{F}(\boldsymbol{\alpha}, <\boldsymbol{\alpha}_v>) - \boldsymbol{\gamma}) \tag{3.51}$$

where

$$\operatorname{cov}(\mathbf{F} - \boldsymbol{\gamma}) = \operatorname{cov}(\boldsymbol{\gamma}) + \nabla_{\boldsymbol{\alpha}_v} \mathbf{F}(\boldsymbol{\alpha}, \boldsymbol{\alpha}_v) \operatorname{cov}(\boldsymbol{\alpha}_v)(\nabla_{\boldsymbol{\alpha}_v} \mathbf{F}(\boldsymbol{\alpha}, \boldsymbol{\alpha}_v))^{\mathrm{T}} \tag{3.52}$$

From the data provided in the tables of the previous section, we find

$$r^2 = 17.5 \tag{3.53}$$

which has a significance of (Hills and Trucano, 2001)

$$\mathrm{P}(\chi^2(10) > r^2) = 0.064 \tag{3.54}$$

Note that we have 10 degrees of freedom since we have 10 measurements. Eq. (3.54) tells us that we have a 6.4% probability of obtaining $r^2 = 17.5$ or larger for a valid model for

the validation experiments. If we choose to test the model at the 5% significance level, then we do not have sufficient evidence to reject the model as valid. Keep in mind that we picked these simulated measurements so that we were near the boundary of model rejection. This is why the significance 6.5% is close to our 5% cut-off point.

The above procedure does not account for the target application. How does this result change if we account for the target application by the representative methods developed in the previous chapter? The metric developed in the previous chapter is given by Eq. (2.43).

$$r^2 = \Delta\mathbf{d}^{\mathrm{T}} \operatorname{cov}^{+}(\mathbf{d})\Delta\mathbf{d} \tag{2.43}$$

where cov(**d**) is given by Eq. (2.42).

$$\operatorname{cov}(\mathbf{d}) = \mathbf{A}^{\mathrm{T}}\left[\operatorname{cov}(\boldsymbol{\gamma}) + \nabla_{\boldsymbol{\alpha}_v}\mathbf{F}(\boldsymbol{\alpha},\boldsymbol{\alpha}_v)\operatorname{cov}(\boldsymbol{\alpha}_v)(\nabla_{\boldsymbol{\alpha}_v}\mathbf{F}(\boldsymbol{\alpha},\boldsymbol{\alpha}_v))^{\mathrm{T}}\right]\mathbf{A} \tag{2.42}$$

The difference in the reconstructed decision variables is give by

$$\Delta\mathbf{d} = \mathbf{A}^{\mathrm{T}}(\mathbf{F}(\boldsymbol{\alpha},<\boldsymbol{\alpha}_v>) - \boldsymbol{\gamma}) \tag{3.55}$$

Note that we evaluate the model for the predicted validation measurements at the expected value of the uncertain model parameters. For highly nonlinear problems, a more appropriate alternative would be to replace $\mathbf{F}(\boldsymbol{\alpha},<\boldsymbol{\alpha}_v>)$ with the expected value of **F**, $<\mathbf{F}(\boldsymbol{\alpha},\boldsymbol{\alpha}_v)>$.

We need to evaluate a pseudoinverse of cov(**d**) since we will find the rank of **d** is not equal to the dimension of **d**. We will also need to evaluate the rank of **d** so that we know the number of degrees of freedom of our resulting metric.

The Mathematica (Woolfram, 1999) routine PseudoInverse implimented here uses the singular value decomposition to find those directions in the row and column spaces of a matrix that have non-zero singular values (related to the eigenvalues). This routine then takes the inverse in just the subspace corresponding to the non-zero singular values. This is discussed in Hills and Trucano (2001). We can perform a singular value decomposition directly to find the number of non-zero singular values using the Mathematic routine SingularValue. The number of non-zero singular values will be equal to the rank of the pseudoinverse matrix provided by PseudoInverse. Applying this process, we found that the cov(**d**) had 4 non-zero singular values (zero within the default tolerance used by Mathematica, Woolfram, 1999), indicating that we have only 4 degrees of freedom in the covariance matrix. This is not surprising since we defined the weighting matrix **A** to best map the validation experiments sensitivity matrices to the decision variable sensitivity matrix. The latter has a rank of 4, the number of important parameters. Thus, we may expect the weighting matrix **A** to map the covariance matrix for the differences between

the validation model predictions and the corresponding experimental measurements into a 4 dimensional subspace. The dimension of this subspace represents the degrees of freedom of our cov(**d**) matrix and should be used for the degrees of freedom for our statistical inference.

Taking the pseudoinverse of cov(**d**), utilizing Eq.(2.43) and the data provided in the tables results in

$$r^2 = \Delta\mathbf{d}^{\mathrm{T}} \operatorname{cov}^{+}(\mathbf{d})\Delta\mathbf{d} = 9.46 \tag{3.56}$$

Since r^2 is distributed as a $\chi^2(n^+)$ with $n^+ = 4$ degrees of freedom, we can evaluate the cumulative probability of obtaining a larger r^2, given that our model is valid. We find

$$\mathrm{P}(\chi^2(4) > r^2) = 0.051 \tag{3.57}$$

This indicates that 5.1% of experiments with a valid model would provide an r^2 this large or larger, given the present levels of uncertainty in the measurements and in the model parameters. Thus, if we wish to evaluate this model at the 5% confidence level (i.e. reject a model only if the probability is less than 5% of observing these or worse results with a valid model), we cannot reject this model as valid. Since we actually used the model to generate this data, we would hope that this model would not be rejected as valid. Note that the probability given by Eq. (3.57) is very close to the probability given when the effect of the target application is not included (i.e., Eq. (3.54)). In this case, the effect of the target application on our metric is not large. This is not too surprising since our target application is very similar to the validation experiments. The most significant differences are 1) the use of surface flux for the decision variable of the target application whereas we used internal temperature measurements for the validation experiments, 2) the denser sampling rate for the target application, and 3) the use of larger times for the target application.

The metric of Eq. (3.56) is defined in terms of a vector of decision variables, the time varying behavior of surface flux for our heat conduction problem. We can also define a metric for each time. In this case, Eq. (3.56) becomes

$$r_i^2 = \Delta d_i^{\,2} / \sigma_i^{\,2} \tag{3.58}$$

where σ_i^2 is the $(i, i)^{\text{th}}$ element in the cov(**d**). Since this is a single variable, the degrees of freedom is one. The results of applying this metric to our data is given in Table 3.6. Note that all of the r^2 are small, the corresponding levels of significance are quite high, and that they are nearly uniform. This indicates that on a point-by-point basis, the corresponding uncertainty in the reconstructed decision variable difference is large. If all we care about is the ability of the validation experiments to represent the decision variable for a single time, then the uncertainty in the corresponding metric is large, and we do not have as

rigorous of a test. If, on the other hand, we care about the ability to represent all of the decision variable times, then we may be tempted to take the product of the individual probabilities (which ignores dependence) given in Table 3.6 to give us the probability of all of the measurements being further from the model predictions. The product is

$$\prod_i \mathrm{P}(\chi^2(1) > r_i^2) = 0.10 \tag{3.59}$$

Note that this is considerably less than the 0.77 values obtained for the point-by-point metrics (Table 3.6). This decreased value for the significance is due to the increase ability to resolve bad models due to the use of multiple data. However, Eq. (3.59) should *not* be used in this fashion. This product does not represent the true significance of the multivariate data because it does not account for correlation between the differences (see Hills and Trucano, 2002). In contrast, Eqs. (3.56) and (3.57) do properly account for the correlation effects and should be used.

Table 3.6: Scalar Decision Variable Metrics

Time	r_i^2	$\mathrm{P}(\chi^2(1) > r_i^2)$
0.125	0.0814	0.78
0.250	0.0785	0.78
0.375	0.0804	0.78
0.500	0.0824	0.77
0.625	0.0835	0.77
0.750	0.0840	0.77
0.875	0.0841	0.77
1.000	0.0842	0.77
10.00	0.0842	0.77

3.6 Transient Heat Conduction with Parameter Uncertainty: Reduced Parameters

The example presented in Section 3.4 demonstrate strong sensitivity to measurement error. This suggests that our unit-to-system experiments are not adequately designed to resolve sensitivity to the 4 parameters listed in Table 3.1. While the thermal conductivity does appear as a separate parameter in the flux boundary condition shown in Eq. (3.45b), heat conduction in the interior of the region is governed by the thermal diffusivity, the ratio of k and ρC_p. Here we repeat the previous example problem, but consider only the three parameters T_0, T_1, and the ratio $k/\rho C_p$ to be the important parameters.

The model equations are given by Eqs. (3.43) through (3.45) where the important and uncertain model parameters are given by the following:

Experiment:	**Application:**
Important: T_0, T_1, $k/\rho C_p$	Important: T_0, T_1, $k/\rho C_p$
Uncertain: $k/\rho C_p$	Uncertain: T_0, T_1, $k/\rho C_p$

In this case, we define the α's as follows:

$$\alpha_1 = T_0, \ \alpha_2 = T_1, \ \alpha_3 = k/\rho C_p \tag{3.60}$$

The unit and system level uncertain parameters are

$$\alpha_{v1} = k \ , \ \alpha_{a1} = T_1, \ \alpha_{a2} = T_2, \ \alpha_{a3} = k/\rho C_p \tag{3.61}$$

The analytical solution to this problem still applies (i.e., Eqs. (3.48) through (3.50)).

The uncertainties in the model parameters, and the measurements, are defined in Table 3.7.

Table 3.7: Model Parameters and Temperature Measurements

Parameter	**Mean Value**	**Standard Deviation**
Validation Experiment		
$k/\rho C_p$	1.0	0.05
γ		0.25
Application		
T_1	10.0	2.0
T_2	20.0	2.0
$k/\rho C_p$	1.0	0.1

In this example, we ignore the uncertainty in k and only consider the uncertainty in the thermal diffusivity $k/\rho C_p$. Here we take k=1. Comparing Tables 3.1 and 3.7, we note that the uncertainty in the validation experiment due to k in Table 3.1 and $k/\rho C_p$ in Table 3.7 will result in the same uncertainty in the model predictions for the validation experiment since k only appears in the ratio $k/\rho C_p$ in the model for the validation experiment. Thus we can use the simulated experimental measurements and model predictions given in Table 3.2.

The process described in Section 3.4 was repeated to estimate the sensitivity coefficients for the validation experiment and the target application. These are tabulated in Tables 3.8 and 3.9.

Table 3.8: Sensitivity Coefficients for Validation Model Parameters

Time	x	$\frac{\partial \mathbf{F}}{\partial T_1}$	$\frac{\partial \mathbf{F}}{\partial T_2}$	$\frac{\partial \mathbf{F}}{\partial\left(\frac{k}{\rho C_p}\right)}$
0.10	0.25	0.5761	0.08834	4.711
0.25	0.25	0.7118	0.2118	2.790
0.50	0.25	0.7468	0.2468	0.4677
0.75	0.25	0.7497	0.2497	0.05877
1.00	0.25	0.7410	0.2500	0.006565
0.10	0.75	0.08834	0.5766	5.186
0.25	0.75	0.2118	0.7118	2.793
0.50	0.75	0.2468	0.7468	0.4677
0.75	0.75	0.2497	0.7497	0.05877
1.00	0.75	0.2500	0.7500	0.006565

Table 3.9: Sensitivity Coefficients for Target Application Model

Time	$\frac{\partial \mathbf{G}}{\partial T_1}$	$\frac{\partial \mathbf{G}}{\partial T_2}$	$\frac{\partial \mathbf{G}}{\partial\left(\frac{k}{\rho C_p}\right)}$
0.125	0.4319	-1.597	22.126
0.250	0.8305	-1.170	12.411
0.375	0.9506	-1.049	5.384
0.500	0.9856	-1.014	2.078
0.625	0.9958	-1.004	0.752
0.750	0.9988	-1.001	0.261
0.875	0.9996	-1.000	0.088
1.000	0.9999	-1.000	0.029
10.00	1.0000	-1.000	0.000

The resulting distribution of uncertainty in the decision variable is provide in Table 3.10. Note that there is considerable less uncertainty for the present 3 parameter case than there was for the previous 4 parameter case. For example, at late times, the estimated standard

deviation is 3.02 for the present case and 51.7 for the 4 parameter case. The validation experiments are much less sensitive to measurement error when we used them to resolve the sensitivity of the models to three parameters rather than four. Because the three parameters do not independently account for thermal conductivity, an additional experiment should be designed and performed to properly test the ability of the model to predict thermal conduction, independent of thermal diffusion. The results of Table 3.10 also indicate that most of the sensitivity in the reconstructed decision variable originate from uncertainties in the model parameters in the target application. This is not unexpected since the uncertainties in the model parameters for the target application are larger than for the validation experiments, as indicated by the values listed in Table 3.7.

Table 3.10: Distribution of Uncertainty in Decision Variable

Time	$\sigma_{d\text{-}meas}$	$\sigma_{d\text{-}v}$	$\sigma_{d\text{-}a}$	σ_d
0.125	0.949	1.106	4.84	5.06
0.250	0.579	0.621	3.47	3.57
0.375	0.381	0.269	3.10	3.14
0.500	0.329	0.104	3.02	3.04
0.625	0.320	0.038	3.01	3.02
0.750	0.318	0.013	3.00	3.02
0.875	0.318	0.004	3.00	3.02
1.000	0.318	0.001	3.00	3.02
10.00	0.318	0.000	3.00	3.02

3.7 Transient Heat Conduction with Parameter Uncertainty: Reduced Parameters - Validation

We now repeat the evaluation of the model validation metric for the 3 parameter case. Using the metric defined by Eqs. (2.43) we find the following (note cov(**d**) now has a rank of 3 since we are dealing with three parameters):

$$r^2 = 9.38; \;\; P(\chi^2(3) > r^2) = 0.025 \qquad (3.62)$$

Assuming that this model is valid, the probability that this model would give the above r^2 or larger is only 2.5%. This suggest that we have good evidence to reject the model as valid. Note that in the previous case of 4 parameters, our level of significance (Eq. (3.57)) was 5.1% rather than 2.5%. This is because the previous experiment has significant uncertainty in the reconstructed decision variable. Since the statistical inference just performed measures the differences between model prediction and experimental

observations relative to the uncertainty in the validation exercise, the larger the uncertainty, the less likely are we to reject a bad model. This result illustrates the importance of sensitivity analysis during the experimental design of validation experiments.

3.8 Two-Dimensional Impact of Aluminum on Aluminum: Representative Method

3.8.1 Background

Before presenting the results of applying the present techniques to the high-speed impact of aluminum on aluminum, a brief review of past validation work for this application will be given.

3.8.2 One-Dimensional Validation

Hills and Trucano (2001) performed a model validation test of CTH predictions for shock wave speed as a function of particle speed for the impact of an aluminum slug on an equal sized, but stationary aluminum slug. CTH is an Eulerian shock physics code developed at Sandia National Laboratories (McGlaun, et. al., 1990, Bell et. al., 1998, Hartel and Kerley, 1998). Shock wave speed versus particle speed (one-half impact speed in this case) data were taken from 232 experiments for this impact (Marsh, 1980). The experiments were designed so that the resulting shocks were one-dimensional and steady.

The 232 data pairs were randomly divided into two groups (see Hills and Trucano, 2001, for a listing of the data). One group of 112 measurements of shock speed versus particle speed was used to calibrate the Mie-Grüneisen Equation of State model used by the CTH code. The form of the shock Hugoniot required by this equation of state is given by (Hartel and Kerley, 1998)

$$U_s = C_S + S_1 U_p + (S_2/C_S) U_p^2 \tag{3.63}$$

where U_s and U_p are shock and particle speeds, respectively. The remaining variables in Eq. (3.63) are material dependent calibration constants. As Hills and Trucano (2001) discussed, there is the expected linear relationship between shock and particle speed for this particular data set over this particular range of data. S_2 is thus zero and a regression analysis on the 112 data pairs was used to estimate C_S and S_1. The results of this analysis provided the following calibration constants and their statistics in the form of a covariance matrix.

$$\boldsymbol{\alpha} = \begin{bmatrix} C_S \\ S_1 \end{bmatrix} = \begin{bmatrix} 5344 \\ 1.305 \end{bmatrix} \tag{3.64a}$$

$$\mathrm{cov}(\boldsymbol{\alpha}) = \begin{bmatrix} 166.4 & -0.0663 \\ -0.0663 & 3.5\times10^{-5} \end{bmatrix} \tag{3.64b}$$

The differences between the U_s of the 112 data U_s-U_p pairs and the regression given by Eqs. (3.63) were then used as an estimate the measurement uncertainty. This estimate is made under the assumption of uniform standard deviation of these differences across all U_p. The estimated standard deviation was found to be

$$\sigma_{exper} = 83.7 \text{ m/s} \tag{3.65}$$

Hills and Trucano (2001) assumed that the measurement uncertainty was uncorrelated. The corresponding covariance matrix for the measurement uncertainty is thus given by

$$\mathrm{cov}(\mathbf{U_{s\_exper}}) = \sigma_{exper}^{\ 2}\, \mathbf{I} \tag{3.66}$$

where **I** is the Identity matrix.

With this model for the uncertainty in the calibration constants, CTH was used to propagate this parameter uncertainty through the model to evaluate the corresponding uncertainty in the predicted shock wave speed for the remaining 120 measurement pairs. These results were then used to test or validate the model. A first-order sensitivity analysis was used to relate the covariance of the model predictions to the covariance of the model parameters (see Hills and Trucano, 2001 for details). The prediction uncertainty, as represented by the covariance matrix, is given by

$$\mathrm{cov}(\mathbf{U_{s\_pred}}) = \nabla_{\boldsymbol{\alpha}}\mathbf{F}(\boldsymbol{\alpha})\,\mathrm{cov}(\boldsymbol{\alpha})(\nabla_{\boldsymbol{\alpha}}\mathbf{F}(\boldsymbol{\alpha}))^{\mathrm{T}} \tag{3.67}$$

where the component values for the gradient are listed in Appendix A for each of the 120 validation data pairs. With models for measurement and prediction uncertainty, a model for the uncertainty of the prediction differences, **p**, was developed.

$$\mathbf{p} = \mathbf{U_{s\_pred}} - \mathbf{U_{s\_exper}} \tag{3.68}$$

The covariance of **p** is given by (Hills and Trucano, 2001)

$$\mathrm{cov}(\mathbf{p}) = \mathrm{cov}(\mathbf{U_{s\_pred}}) + \mathrm{cov}(\mathbf{U_{s\_exper}}) \tag{3.69}$$

The assumption that the error distributions were multi-normal with the above covariance matrix defines the 120 dimensional PDF cloud for the validation exercise. The total uncertainty was dominated by measurement uncertainty (see Hills and Trucano, 2001), so the PDF cloud was nearly spherical in shape. Curves of iso-probability for multi-normal PDF are given by constant r^2 values for the following quadratic equation

$$r^2 = \begin{bmatrix} p_1 - p_{mean1} & p_2 - p_{mean2} & \cdots & p_{120} - p_{mean120} \end{bmatrix} \mathrm{cov}^{-1}(\mathbf{p}) \begin{bmatrix} p_1 - p_{mean1} \\ p_2 - p_{mean2} \\ \vdots \\ p_{120} - p_{mean120} \end{bmatrix} \quad (3.70)$$

The validation hypothesis was that the mean prediction difference for each measurement location was zero. For this case Eq. (3.70) becomes

$$r^2 = \begin{bmatrix} p_1 & p_2 & \cdots & p_{120} \end{bmatrix} \mathrm{cov}^{-1}(\mathbf{p}) \begin{bmatrix} p_1 \\ p_2 \\ \vdots \\ p_{120} \end{bmatrix} \quad (3.71)$$

From the estimated covariance matrix for the validation exercise and the prediction errors, Hills and Trucano (2001) found that

$$r^2 = 130.0 \quad (3.72)$$

The cumulative probability for some r^2 in this PDF cloud is given by the χ^2 distribution with 120 degrees of freedom corresponding to the 120 measurement pairs (see Hills and Trucano, 2001). The critical value of r^2 for which 5% of the cumulative probability is outside the r^2 = constant PDF surface is

$$r^2_{\mathrm{critical}} = \chi^2_{0.95}(120) = 146.6 \quad (3.73)$$

Since r^2 = 130.0 is less than 146.6, the hypothesis that the mean prediction difference is zero, could not be rejected at the 95% confidence level. The data does not provide statistically significant evidence that the model is invalid.

3.8.3 Two-Dimensional Target Application: Projection Method

Hills and Trucano (2001) developed an application-based metric for the two-dimensional impact of a small 1 cm diameter cylindrical aluminum slug on a much larger 10 cm diameter aluminum cylinder. In the present report, this approach is called the projection method and was summarized in the previous chapter. The two-dimensional geometry of the application results in non-steady shock waves, with variable shock speeds throughout the larger aluminum cylinder. Conservation of momentum applied to the spherically expanding shock wave requires that shock speed decrease with time. Here we take this two-dimensional application as the target application and consider the one-dimensional

data presented in the previous section as the unit level measurements.

The integrated decision variable was chosen to be the transit time for the shock wave to arrive at the back side of the larger aluminum cylinder. This time was defined as the time the particle speed on the back surface of the larger cylinder reaches 250 m/s with a front side impact speed of 6000 m/s. This impact speed produces a maximum particle speed of 3000 m/s (see Hills and Trucano, 2001). In contrast, the validation experimental data covers a particle speed range from approximately 300 m/s to 4400 m/s. Since particle speeds are 3000 m/s or less for the two-dimensional case, only a subset of the experimental data was used in the analysis. Of the 120 U_p-U_s pairs selected for validation, 89 covered the range from 0 – 3100 m/s. These data pairs are listed in Appendix A. Only those data pairs within this range of U_p were used in the following analysis.

Uncertainty in predicting the shock transit time results from the uncertainty in the two model parameters C_S and S_1 used in CTH. A sensitivity analysis was used to develop a mapping between the model parameters and the application decision variable (transit time). Since there was just one decision variable and two model parameters, the sensitivity matrix has one row and two columns. This sensitivity matrix was used to determine a direction in the model parameter space that has no effect on the decision variable (i.e., the projection method of the previous chapter). Hills and Trucano (2001) found this matrix to be

$$\nabla_{\alpha}\mathbf{G}(\boldsymbol{\alpha}) = \left[-1.155\text{x}10^{-9} \quad 4.7034\text{x}10^{-7}\right] \tag{3.74}$$

This in turn provided a means to exclude prediction-measurement differences in the direction that does not impact on the decision variable using the projection method presented in Chapter 2.

The result of this approach (see Hills and Trucano, 2001) was to project the 89-dimensional validation data space into an 88-dimensional space. As discussed earlier, the covariance matrix based on this projection requires a pseudo-inverse to be performed because the inverse does not exist in the full 89-dimensional space. As in the previous section, we tested the hypothesis that the mean prediction difference for each measurement location was zero. This time the projected quantities were used, denoted by a superscript p. Analogous to Eq. (3.68), we have

$$\mathbf{p} = \mathbf{P}(\mathbf{U}_{\text{s\_pred}} - \mathbf{U}_{\text{s\_exper}}) = \mathbf{U}^{\mathbf{p}}_{\text{s\_pred}} - \mathbf{U}^{\mathbf{p}}_{\text{s\_exper}} \tag{3.75}$$

where the projection matrix $\mathbf{P}$ is given by Eq. (2.9).

The covariance matrix of $\mathbf{p}$ was taken to be

$$\text{cov}(\mathbf{p}) = \mathbf{P}\,\text{cov}(\mathbf{U}_{\text{s\_pred}})\mathbf{P}^{\text{T}} + \mathbf{P}\,\text{cov}(\mathbf{U}_{\text{s\_exper}})\mathbf{P}^{\text{T}} = \text{cov}(\mathbf{U}^{\mathbf{p}}_{\text{s\_pred}}) + \text{cov}(\mathbf{U}^{\mathbf{p}}_{\text{s\_exper}}) \tag{3.76}$$

The pseudo-inverse of the covariance matrix is designated $\text{cov}^{+}(\mathbf{p})$. Our metric for the subspace in terms of the pseudo-inverse is an analogous expression to Eq. (3.71).

$$r^2 = \begin{bmatrix} p_1 & p_2 & \cdots & p_{89} \end{bmatrix} \text{cov}^{+}(\mathbf{p}) \begin{bmatrix} p_1 \\ p_2 \\ \vdots \\ p_{89} \end{bmatrix} \tag{3.77}$$

Evaluation of Eq. (3.77) for the 89 model predictions and experimental measurements gave

$$r^2 = 54.7 \tag{3.78}$$

A statistical test for the probability of this measure of prediction measurements was based on the χ^2 distribution with 88 degrees of freedom. A critical value of r^2 for which the cumulative probability inside the corresponding PDF surface is 95% is

$$r^2_{\text{critical}} = \chi^2_{0.95}(88) = 110.9 \tag{3.79}$$

Since $r^2 = 54.7$ is less than 110.9, there was no statistical evidence to reject the model (CTH) as being invalid at the 95% confidence level which corresponds to a 5% level of significance.

In this section, we presented an overview of the projection method based, application specific metric, which was originally developed by Hills and Trucano (2001) and applied to shock physics data. In the next section, we use the alternative representative method to develop the weights and the metric. We return to the projection method based metric for non-normally distributed CTH model parameters in a later section.

3.8.4 Two-Dimensional Target Application: Representative Method

The representative method defined in Chapter 2 is now applied to the aluminum impact case described above. As stated previously, the decision variable is the shock transit time, $d=\tau$, the particle velocity on the back side of the large cylinder is anticipated to reach 250 m/s. In contrast to the projection method example, we will use all 120 measurements, rather than the previously specified 89-measurement subset. Since this is a single decision variable, we will denote the vector $(\nabla_{\alpha}\mathbf{G}(\boldsymbol{\alpha},\boldsymbol{\alpha}_a))^{\text{T}}$ as $\mathbf{g}$.

$$\mathbf{g} = \left(\nabla_{\alpha}\mathbf{G}(\boldsymbol{\alpha},\boldsymbol{\alpha}_a)\right)^{\text{T}} \tag{3.80}$$

The components of $\mathbf{g}$ are given in Eq. (3.74). Eq. (2.35) is used to evaluate the weights to be used on the measurements to reflect the application.

$$\mathbf{a} = \left(\text{cov}(\mathbf{F}-\boldsymbol{\gamma})\right)^{-1} \quad (\nabla_{\boldsymbol{\alpha}}\mathbf{F}(\boldsymbol{\alpha},\boldsymbol{\alpha}_v))\times \\ \left((\nabla_{\boldsymbol{\alpha}}\mathbf{F}(\boldsymbol{\alpha},\boldsymbol{\alpha}_v))^{\mathrm{T}}\left(\text{cov}(\mathbf{F}-\boldsymbol{\gamma})\right)^{-1} \quad (\nabla_{\boldsymbol{\alpha}}\mathbf{F}(\boldsymbol{\alpha},\boldsymbol{\alpha}_v))\right)^{-1}\mathbf{g} \tag{3.81}$$

where a lower case **a** is used to reflect that we have a single decision variable. The covariance in the differences between the model predictions and the experimental observations is given by Eq. (2.36)

$$\text{cov}(\mathbf{F}-\boldsymbol{\gamma}) = \text{cov}(\boldsymbol{\gamma}) + \nabla_{\alpha_v}\mathbf{F}(\boldsymbol{\alpha},\boldsymbol{\alpha}_v)\,\text{cov}(\boldsymbol{\alpha}_v)\nabla_{\alpha_v}\mathbf{F}(\boldsymbol{\alpha},\boldsymbol{\alpha}_v)^{\mathrm{T}} \tag{3.82}$$

where the covariance matrix for the measurements is given by Eq. (3.66).

$$\text{cov}(\boldsymbol{\gamma}) = \text{cov}(\mathbf{U}_{\mathbf{s\_exper}}) = \sigma_{\text{exper}}^2\,\mathbf{I} \tag{3.83}$$

The covariance matrix for the model parameters is given by Eq. (3.64b). The gradient term for the validation model is given by

$$\nabla_{\alpha}\mathbf{F}(\boldsymbol{\alpha},\boldsymbol{\alpha}_{\mathrm{v}}) = \begin{bmatrix} \dfrac{\partial U_{S_1}}{\partial C_s} & \dfrac{\partial U_{S_1}}{\partial S_1} \\ \dfrac{\partial U_{S_2}}{\partial C_s} & \dfrac{\partial U_{S_2}}{\partial S_1} \\ \vdots & \vdots \\ \dfrac{\partial U_{S_{120}}}{\partial C_s} & \dfrac{\partial U_{S_{120}}}{\partial S_1} \end{bmatrix} \tag{3.84}$$

where the components of this matrix are provide in Appendix A for the 120 measurement pairs. The terms in Eq. (3.81) are now completely defined. Evaluating this equation results in the weights listed in Table 3.11 (note the pre-scaling of 10^{12}) and plotted in Figure 3.4.

The uncertainty in the reconstructed decision variable including the effect of target application parameter uncertainty, expressed as the covariance of **d**, can be found by application of Eq. (2.39).

$$\text{cov}(d) = \mathbf{a}^{\mathrm{T}}\left[\text{cov}(\boldsymbol{\gamma}) + \nabla_{\boldsymbol{\alpha}_v}\mathbf{F}(\boldsymbol{\alpha},\boldsymbol{\alpha}_v)\,\text{cov}(\boldsymbol{\alpha}_v)(\nabla_{\boldsymbol{\alpha}_v}\mathbf{F}(\boldsymbol{\alpha},\boldsymbol{\alpha}_v))^{\mathrm{T}}\right]\mathbf{a} + \mathbf{g}\,\text{cov}(\boldsymbol{\alpha}_a)\mathbf{g}^{\mathrm{T}} \tag{3.85}$$

Evaluating Eq. (3.85) results in

$$\text{cov}(\tau) = \text{cov}(d) = 7.279\text{x}10^{-16}\ (\text{sec})^2 \tag{3.86}$$

The standard deviation is simply

$$\sigma_\tau = \sqrt{\text{cov}(\tau)} = 2.7 \times 10^{-8} \text{ sec} \tag{3.87}$$

A calculated time of arrival for the shock on the backside of the large aluminum block can be estimated from Fig 3.14 in Hills and Trucano (2001). The estimate, based on a simple curve fit of time versus shock front location, indicates a transit time for the leading edge of the shock of 7.6×10^{-6} sec. The reconstructed uncertainty ($2\sigma_\tau$) amounts to approximately 0.7 % of the transit time. This small uncertainty is consistent with the two-dimensional validation metric reviewed above.

We can now use the weighting vector of Table 3.11 to develop the corresponding validation metric using the methodology of Sections 2.3.1 and 2.3.2. Eq. (2.42) and (2.43) can be written as

$$\text{cov}(d) = \mathbf{a}^{\text{T}} \left(\text{cov}(\boldsymbol{\gamma}) + \nabla_{\boldsymbol{\alpha}_v} \mathbf{F}(\boldsymbol{\alpha}, \boldsymbol{\alpha}_v) \, \text{cov}(\boldsymbol{\alpha}_v) (\nabla_{\boldsymbol{\alpha}_v} \mathbf{F}(\boldsymbol{\alpha}, \boldsymbol{\alpha}_v))^{\text{T}} \right) \mathbf{a} \tag{3.88}$$

and

$$r^2 = \Delta d^2 / \text{cov}(d) \tag{3.89}$$

since we have only one decision variable. Our Δd is given by

$$\Delta d = \mathbf{a}^{\text{T}} \left(\mathbf{U}_{\text{p\_pred}} - \mathbf{U}_{\text{s\_meas}} \right) \tag{3.90}$$

where the model predictions and experimental measurements are given in Table A.1. Evaluating Eq. (3.89) gives

$$r^2 = 0.1670 \tag{3.91}$$

The probability that we can obtain this value or a larger value for r^2 is

$$P(\chi^2(1) > r^2) = 0.683 \tag{3.92}$$

Thus, we have a 68% probability of this r^2 or a larger value, given that the model is valid. Since we would generally not reject a model as valid unless this percentage is less than 5%, we do not have sufficient statistical evidence to reject this model.

Table 3.11: The Weighting Vector for the Shock Physics Data

Up	$a_i \times 10^{12}$	Up	$a_i \times 10^{12}$	Up	$a_i \times 10^{12}$
278	-40.48	1121	-25.44	2738	3.17
440	-37.24	1128	-24.99	2817	5.07
472	-36.83	1130	-24.93	2911	7.36
503	-36.38	1134	-24.83	2935	7.83
507	-36.38	1136	-25.04	2974	7.67
609	-34.46	1141	-24.98	2987	6.88
626	-34.31	1159	-24.44	3030	7.44
627	-34.29	1220	-23.63	3031	7.48
671	-33.36	1220	-23.63	3086	11.85
722	-32.25	1277	-22.34	3181	10.25
727	-32.38	1352	-20.70	3187	10.35
728	-32.37	1383	-20.12	3217	11.54
778	-31.53	1437	-19.51	3225	13.73
786	-31.14	1446	-18.73	3238	14.07
792	-31.11	1467	-18.57	3260	14.39
792	-31.11	1498	-19.27	3274	14.59
799	-31.13	1557	-16.76	3347	13.36
800	-31.22	1574	-16.72	3361	13.89
800	-31.22	1578	-16.91	3376	13.34
802	-31.15	1605	-16.28	3381	13.99
802	-31.15	1742	-13.61	3387	14.08
809	-30.76	1744	-13.72	3400	16.15
818	-30.70	1779	-13.65	3419	16.64
831	-30.62	1858	-11.76	3463	17.86
859	-29.99	1939	-10.34	3472	18.15
863	-29.85	1948	-9.89	3481	18.04
871	-29.55	1959	-10.59	3508	17.56
888	-29.64	2154	-7.21	3508	17.56
891	-29.56	2156	-7.17	3563	18.34
896	-29.36	2335	-2.74	3629	20.98
897	-29.36	2371	-2.12	3658	21.37
901	-29.24	2467	-0.61	3736	20.31
953	-28.21	2477	-0.74	3745	21.80
953	-28.21	2595	1.58	3772	20.73
966	-28.08	2605	1.00	3786	23.06
975	-28.22	2608	1.99	3930	24.50
988	-27.77	2641	2.22	3967	24.37
1110	-25.64	2645	2.13	3988	26.49
1116	-25.53	2709	1.90	4001	26.40
1119	-25.49	2735	3.76	4041	28.71

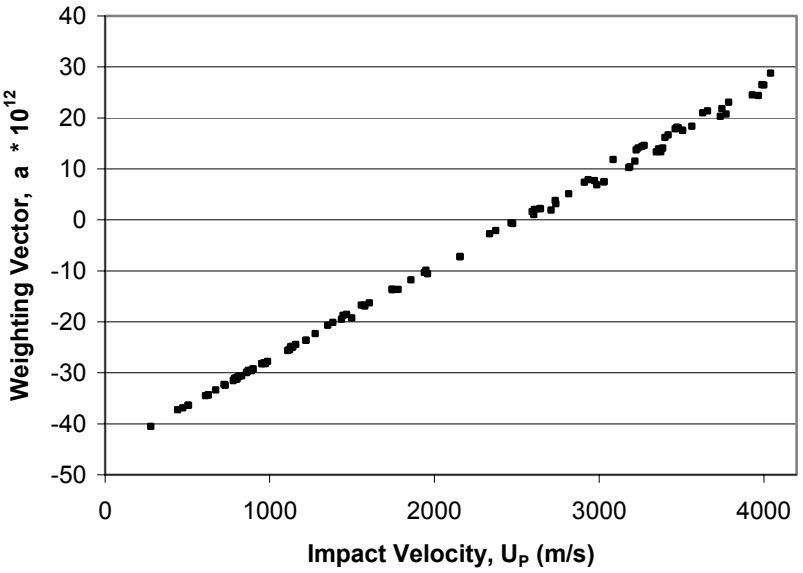

Figure 3.4: Weighting factors for 1-D CTH results applied to 2-D application.

3.9 CTH Example: Representative Method for Non-Normal Distribution

We end this chapter with the example application using the Maximum Likelihood method to develop a metric, using non-normal distributions in the model parameters. This approach was developed by Gaultney (2001) and repeated here with different statistical parameters. In contrast to the previous section, we use the projection method (see Chapter 2) to develop the weights. For demonstration purposes, we use the following CTH model parameters and distributions.

The uncertainty in the measurements **d** are assumed to be uncorrelated. The Beta and Triangular distributions are given by

$$\mathrm{PDF}_{\mathrm{beta}}(x_b) = \begin{cases} \dfrac{\Gamma(\beta_1+\beta_2)}{\Gamma(\beta_1)\Gamma(\beta_1)} x_b^{\beta_1-1}(1-x_b)^{\beta_2-1}, & 0 < x_b < 1 \\ 0, \quad \text{otherwise} \end{cases} \tag{3.93a}$$

where

$$x_b = \frac{\alpha_1 - \alpha_{1,lb}}{\alpha_{1,ub} - \alpha_{1,lb}} \tag{3.93b}$$

Table 3.12: Distributions for Measurements and Model Parameters

Variable	Distribution	Parameter	Value
α_1 (Cs)	Beta	$\alpha_{1,lb}$	5318 m/s
		$\alpha_{1,ub}$	5370 m/s
		$\beta 1$	3
		$\beta 2$	2
α_2 (S1)	Triangular	$\alpha_{2,lb}$	1.293
		$\alpha_{2,ub}$	1.317
d	Normal	<d>	f(**α**)
		σ_d	83.7

The relevant equations for the normalized triangular distribution assumed for α_2 are

$$\text{PDF}_{\text{traiagular}}(x_t) = \begin{cases} 4x_t, & 0 < x_t \le 0.5 \\ 4(1 - x_t), & 0.5 < x_t \le 1.0 \\ 0, & \text{otherwise} \end{cases} \tag{3.94a}$$

where

$$x_t = \frac{\alpha_2 - \alpha_{2,lb}}{\alpha_{2,ub} - \alpha_{2,lb}} \tag{3.94b}$$

The joint probability density function is given by

$$\text{PDF}(\boldsymbol{\alpha}, \mathbf{Pd}) = \text{PDF}_{\text{beta}}(\alpha_1) \cdot \text{PDF}_{\text{triangular}}(\alpha_2) \cdot \text{PDF}_{\text{normal}}(\mathbf{Pd}) \tag{3.95}$$

We see that we need to know the probability density function for the projected measurements, **Pd**. Because the experimental data are normally distributed, the projected data, **Pd**, will be multinormally distributed. Linear combinations of normally distributed random variables are also normally distributed with the following covariance matrix.

$$\mathbf{V}_d^p = \mathbf{P}\,\mathbf{V}_d\,\mathbf{P}^T \tag{3.96}$$

The covariance matrix for the measurements is given by (see Table 3.12)

$$\mathbf{V}_d = \mathbf{I} * 83.7^2 \tag{3.97}$$

where **I** is the identity matrix since the measure errors are uncorrelated. We can now write the PDF for the projected measurements.

$$\text{PDF}(\mathbf{Pd}) = \frac{1}{\sqrt{(2\pi)^n}\sqrt{\left|\mathbf{V}_d^p\right|}} \exp(-(\mathbf{Pd} - <\mathbf{Pd}>)^T \left(\mathbf{V}_d^p\right)^+ (\mathbf{Pd} - <\mathbf{Pd}>)/2) \tag{3.98}$$

Note that we use the pseudoinverse since the projected covariance matrix will be singular. Gaultney (2001) assumed that when the true values of the model parameters are used, the model will provide predictions that are consistent with the expected value of the measurements.

$$<\mathbf{P}\,\mathbf{d}> = \mathbf{P}\,\mathbf{f}(\boldsymbol{\alpha}) \tag{3.99}$$

Equation (3.98) can now be written

$$\text{PDF}(\mathbf{Pd}) = \frac{1}{\sqrt{(2\pi)^n}\sqrt{\left|\mathbf{V}_d^p\right|}} \exp(-(\mathbf{Pd} - \mathbf{P}\,\mathbf{f}(\boldsymbol{\alpha}))^T \left(\mathbf{V}_d^p\right)^+ (\mathbf{Pd} - \mathbf{P}\,\mathbf{f}(\boldsymbol{\alpha}))/2) \tag{3.100}$$

Rather than re-run CTH, we use the sensitivity matrix already found to approximate the response of the shock speed as a function of particle speed. This is a good approximation since shock speed is linear in the model parameters over the measurement range of interest (see Hills and Trucano, 2001). Our approximate model for the predicted measurements is given by (see Eq. (2.4))

$$\mathbf{f}(\boldsymbol{\alpha}) \approx \mathbf{f}(\boldsymbol{\alpha}_0) + \nabla_{\boldsymbol{\alpha}}\mathbf{F}(\boldsymbol{\alpha})(\boldsymbol{\alpha} - \boldsymbol{\alpha}_0) \tag{3.101}$$

were the components of $\boldsymbol{\chi}$ are the values approximated by Hills and Trucano (2001) and reproduced in Eq. (3.64a), (i.e., $\boldsymbol{\alpha}_0 = [5344, 1.305]^T$).

Given the distributions defined by Eqs. (3.93) through (3.94), we can now choose the model parameters that minimize Eq. (3.95). We use the Mathematica (Woolfram, 1999) optimization routine FindMinimum. As was the case for Gaultney (2001), we use only the 89 measurement subset that was used in Section 3.8.3. The results of this procedure are given in Table 3.13.

Table 3.13: Results of Maximum Likelihood Optimization

Parameter	Value
α_1 (C_s)	5350.1
α_2 (S_1)	1.305

We now need to evaluate the cumulative probability that a valid model will give the corresponding PDF value or less. Because we are dealing with non-normal distributions, Gaultney used a simple Monte Carlo approach. Random values for the measurements are generated using the PDFs, the statistics provided in Table 3.12, and the methodology defined at the end of the previous chapter. These values are substituted into Eq. (3.95) to find the corresponding PDF. This process was repeated 50,000 times resulting in 49,907 of the PDF values being less than that found by the optimization procedure. Thus, we can estimate the significance of the results listed in Table 3.13 as 0.998 (=49,907/50,000). Clearly there is no evidence to reject the CTH model as valid based on the projected measurements as 99.8% is much greater than 5% significance level that we typically use to reject a model (see Hills and Trucano, 2001).

Note that we can apply this same procedure to the weighted measurements, whether they are formed by the projection method or by the Lagrangian weights of the representative method.

(Page left blank)

4.0 Discussion and Recommendations

4.1 Discussion

Several methods have been presented that weight the validation measurement data to better reflect a target application of a model. These methods are based on a first order sensitivity analysis of the models for the validation experiments and for the target application. The first method is Gaultney's (2001) extension of the application-based metric of Hills and Trucano (2001), which removes those directions of the validation space that are not important to the target application. We call this method the projection method since it projects the measurements onto a subspace that does not include the non-relevant direction. Hills and Trucano (2001) demonstrated this metric assuming the model parameters were normally distributed for one-dimensional shock physics validation data with a two-dimensional shock physics application problem. In the present work, we reproduce Gaultney's extension of this metric for non-normally distributed model parameters using a Maximum Likelihood/Monte Carlo method. Hills and Trucano (2002) showed that the Maximum Likelihood approach gives the same results as the r^2 metric developed by Hills and Trucano (2001) for normally distributed measurements and model parameters, and for a model that is locally linear in the parameters. While this method does tend to weigh the more important directions in the validation space more, the weighing is not optimized from a target application point of view.

A second method presented here is based on weighting the measurements in a fashion so that they reflect the target application. We call this the representation method since we use the validation experimental measurements to represent the target application decision variable. This has the effect of not only throwing out the directions in the validation space that are not important to the application, but also weighting the remaining directions based on their importance. The implementation of the method, as presented here, does require that the validation experiments cover the target application in the sense illustrated in the report. More specifically, the validation experiments collectively must be sensitive to the same parameters as is the target application. For example, if heat conduction is important to a transient target application decision variable, then the target application decision variable will be dependent on the thermal diffusivity. If the validation experiments are not dependent on thermal diffusivity, then the validation experiments do not reflect the target application and weights cannot be developed.

The representative method also allows us to evaluate the sensitivity of the target application decision variable to the validation measurements. If the decision variable is not dependent on the same model parameters as the validation experiments or suite of experiments, then the target application is not covered by the validation experiments and additional experiments must be developed. In contrast, if the decision variables are overly sensitive to small differences in the measurements, then the decision variable will be

overly sensitive to noise in the measurements. In this case, we must make sure that the experiments are designed so that noise is sufficiently small.

In the case of more validation measurements than important model parameters, we have the luxury of weighting these measurements so that the decision variable is not as sensitive to measurement noise, while still representing the target application. In doing so, we still must require that the validation experiments provide adequate coverage of the target application. For example, if we have several temperature measurements at the same distance from a boundary in a one-dimensional heat conducting slab, then the present methodology will take a weighted average of these multiple measurements. This averaging reduces the effect of noise in the measurements.

The third approach developed here is an extension of the representative method just discussed that also includes the effect of uncertainty in the model parameters for the validation experiments, as well as the measurements. As in the previous case, this method weights the measurements such that the weighted measurements represent the target application decision variable, while being minimally sensitivity to measurement *and* validation model parameter uncertainties.

These methods were applied to a series of heat conduction problems and to shock physics data. In one example, for which internal heat generation was important, we found that if internal heat generation was not included in the validation experiments, the representative method could detect this lack of coverage. However, we also found that simply performing an experiment that did have internal generation was not, in itself, adequate to resolve the target application decision variable. By including additional heat conduction experiments, our validation experiments did cover the application. Unfortunately, even though the target application decision variable could be represented by the validation experiments, the representation was very sensitive to measurement noise. We showed that the sensitivity could be reduced by properly locating the internal measurements or by providing additional measurements. Thus, we see that the methodology developed here can also be used for experimental design, accounting for the impact of the anticipated target application.

All of these methods require that we identify the model parameters that are important to the target application. Failure to do so can result in incorrect representation of the physics of the target application. For example, in the development of the transient heat conduction example problem for this report, we initially assumed (not presented here) that the important model parameters were the boundary temperatures and the conductivity. However, when we did not get the transient behavior we expected, we realized that we must also include either thermal diffusivity or the density-heat capacity product. The method failed to detect that the validation experiments did not cover this important aspect of transient heat conduction because we did not initially choose thermal diffusivity as an important model parameter for the target application. Methods of this type cannot replace engineering judgment. However, these methods can quantify the

results of this judgment, which will greatly facilitate consensus building concerning the validity of the model. This is a very important outcome for any validation activity.

Finally, we note that all of these methods can be used to develop application-based model validation metrics. We demonstrated such metrics using the projection method for non-normal distributions and using the representation method for normal distributions. As discussed in the previous two chapters, both methods can be applied to non-normal distributions in the model parameters using the Maximum Likelihood method.

4.2 Recommendations

Of the three methods, we suggest that the representative method that addresses uncertainty in both the measurements and in the model parameters for the validation experiment, has the most potential. This method 1) looks at the coverage of the target application decision variables, 2) provides an indication as to how well the decision variables of the target application are represented by the validation experiments, and 3) provides an assessment of the sensitivity of this representation to uncertainty in the measurements and in the model parameters. While this method, as applied here, requires that the suite of validation experiments cover the target application, we suggest (not shown here) that this method can be modified so that it can also apply to target applications not adequately covered by the validation experiments. In the present context, inadequate coverage occurs when the sensitivities of the target application decision variable to the important model parameters are not reflected in the validation experiments. The representative method can be modified to be applicable to this situation by either ignoring the model parameters that are important to the target application, but not represented in the validation experiments; or by using a pseudo-inverse to delete the effect of these directions. In either case, we should look at the results as an indication of the sensitivity of the target application decision variables to only those model parameters that are represented. We must keep in mind that if the suite of validation experiments does not adequately cover the physics of the target application (i.e., possess the appropriate sensitivities), then we will not know what the effect of the missing physics is on our representation of the target application.

This report represents the fourth in a series of reports developed by the present authors (see Hills and Trucano, 1999, 2001, 2002). We suggest that much progress has been made in understanding how to incorporate uncertainty in model parameters and noise in the measurements into model validation metrics. We also have developed a clearer understanding on how to relate validation experiments to target applications. However, we also suggest that the application of these metrics to problems of interest to Sandia National Laboratories has not kept pace with the mathematical development. Part of the reason for the lack of focus on real problems has been due to the need to develop an adequate suite of validation tools that are necessary to rigorously test models against data, and because there were very significant outstanding issues (such as the question of how suites of experiments at the unit level should be combined to represent a target

application). With the completion of this report, we strongly recommend that we return our focus to applications of this methodology to existing applications of interest to Sandia National Laboratories.

5.0 References

Bell, R. L., M. R. Baer, R. M. Brannon, M. G. Elrick, E. S. Hertel, Jr., S. A. Silling, and P. A. Taylor (1998), "CTH User's Manual and Input Instructions, Version 4.0," Sandia National Laboratories, Albuquerque.

Carslaw, H. S., and J. C. Jaeger (1978), Conduction of Heat in Solids, Oxford University Press, New York.

Gaultney, S. E. (2001), Statistical Validation of Engineering and Scientific Models: An Application Based Metric Based on Maximum Likelihood Estimations, M. S. Thesis, Mechanical Engineering, New Mexico State University.

Hertel, E. S. Jr., and G. I. Kerley (1998), "CTH EOS Package: Introductory Tutorial," Sandia National Laboratories, SAND98-0945.

Hills, R. G. and T. G. Trucano (1999), **"**Statistical Validation of Engineering and Scientific Models: Background," Sandia National Laboratories, SAND99-1256.

Hills, R. G.and T. G. Trucano (2001), "Statistical Validation of Engineering and Scientific Models with Application to CTH," Sandia National Laboratories, SAND2001-0312.

Hills, R. G.and T. G. Trucano (2002), "Statistical Validation of Engineering and Scientific Models: A Maximum Likelihood Based Metric," Sandia National Laboratories, SAND2001-1783.

Marsh, S. P., ed. (1980), LASL Shock Hugoniot Data, University of California Press, Berkley.

McGlaun, J. M., S. L. Thompson, and M. G. Elrick (1990), "CTH: A Three-Dimensional Shock Wave Physics Code," Int. J. Impact Engng., Vol. 10, No. 1-4, pp. 351-360.

Strang, G. (1976), Linear Algebra and Its Applications, Academic Press, New York.

Trucano, T. G., R. G. Easterling, K. J. Dowding, T. L. Paez, A. Urbina, V. J. Romero, B. M. Rutherford, and R. G. Hills (2001), "Description of the Sandia Validation Metrics Project," SAND2001-1339, Sandia National Laboratories, Albuquerque, New Mexico, Printed August 2001.

Trucano, T. G., M. Pilch, and W. L. Oberkampf (2002), "General Concepts for Experimental Validation of ASCI Code Applications," SAND2002-0341, Sandia

National Laboratories, Albuquerque, New Mexico, Printed March 2002.

Woolfram, S. (1999), The Mathematica Book, Cambridge University Press, New York.

Appendix A. Shock Physics Data

The shock physics data used by Hills and Trucano (2001) are reproduced in Table A.1 for completeness. The first 2 columns of this data were taken from Marsh (1980). The remaining columns were evaluated using CTH (Bell et. al., 1998, Hertel and Kerley, 1998, McGlaun et. al., 1990), a Eulerian shock physics code. We also show the derivatives (sensitivity coefficients) for the predicted measurements as a function of two model parameters (C_S, S_1) that appear in the Mie-Gruniesen Equation of State model used by the CTH code (Hertel and Kerley, 1998).

Table A.1: Shock Physics Data, CTH Predictions, and Sensitivity Coefficients

Up	Us_exper	Us_pred	$\frac{\partial Us}{\partial C_S}$	$\frac{\partial Us}{\partial S_1}$
278	5811	5731.7	1.00337	276.63
440	6021	5946.5	1.00355	451.34
472	6054	5988.3	1.00412	475.10
503	5996	6030.1	1.00337	497.32
507	6055	6035.4	1.00337	497.32
609	6103	6170.0	1.00225	597.70
626	6262	6192.8	1.00393	609.96
627	6228	6194.1	1.00374	610.73
671	6164	6252.0	1.00187	655.94
722	6367	6319.4	1.00468	722.61
727	6323	6326.5	1.00412	714.18
728	6310	6327.9	1.00412	714.94
778	6388	6394.0	1.00037	750.96
786	6312	6403.1	1.00805	790.80
792	6314	6412.3	1.00580	786.97
792	6365	6412.3	1.00580	786.97
799	6353	6420.7	1.00730	789.27
800	6393	6422.1	1.00730	784.67
800	6459	6422.1	1.00730	784.67
802	6397	6424.8	1.00711	787.74
802	6355	6424.8	1.00711	787.74
809	6422	6433.2	1.00655	807.66
818	6366	6445.9	1.00412	804.60
831	6436	6461.8	1.00823	819.16
859	6470	6500.1	1.00636	848.27
863	6486	6505.3	1.00599	855.17
871	6561	6515.8	1.00468	868.20
888	6541	6537.8	1.00636	867.43
891	6589	6541.8	1.00655	872.03
896	6589	6547.0	1.00936	889.66
897	6579	6548.3	1.00954	890.42
901	6402	6553.7	1.00954	896.55
953	6616	6624.0	1.00037	929.50

953	6617	6624.0	1.00037	929.50
966	6659	6639.6	1.00898	957.85
975	6607	6652.1	1.00730	946.36
988	6507	6667.9	1.00730	970.12
1110	6844	6830.4	1.00318	1075.10
1116	6843	6838.4	1.00374	1081.99
1119	6846	6842.4	1.00393	1085.06
1121	6840	6845.0	1.00412	1088.12
1128	6756	6852.1	1.00430	1112.64
1130	6823	6854.8	1.00430	1115.71
1134	6826	6860.2	1.00393	1120.30
1136	6831	6863.0	1.00374	1108.81
1141	6795	6869.7	1.00355	1111.11
1159	6915	6892.7	1.01010	1156.32
1220	6981	6974.4	1.00225	1180.84
1220	7014	6974.4	1.00225	1180.84
1277	6943	7047.5	1.01048	1270.50
1352	7092	7145.3	1.00674	1349.43
1383	7225	7187.8	0.99663	1356.32
1437	7156	7257.4	1.00805	1416.86
1446	7211	7270.1	0.99869	1436.01
1467	7305	7296.2	1.00543	1461.30
1498	7342	7339.6	1.00225	1415.32
1557	7462	7409.8	1.01516	1582.38
1574	7426	7438.4	0.99551	1536.40
1578	7326	7443.2	1.00337	1545.59
1605	7407	7479.1	0.99345	1554.79
1742	7690	7654.0	1.01796	1758.62
1744	7616	7659.3	1.01291	1740.23
1779	7758	7708.4	1.00225	1718.01
1858	7850	7809.0	1.00879	1836.02
1939	7773	7915.6	1.00580	1904.98
1948	7973	7927.8	0.99626	1905.75
1959	8015	7943.1	1.00318	1885.06
2154	8150	8199.8	1.00767	2078.16
2156	8332	8202.4	1.00748	2079.69
2335	8421	8432.7	1.00580	2314.18
2371	8436	8476.9	1.00468	2344.83
2467	8699	8602.9	1.01553	2452.87
2477	8618	8616.4	1.01628	2447.51
2595	8829	8771.9	1.00281	2539.46
2605	8744	8785.7	1.01497	2537.93
2608	8664	8789.9	1.01478	2590.80
2641	8848	8830.3	1.01329	2599.24
2645	8797	8835.6	1.01385	2596.17
2709	8792	8926.9	0.99083	2527.20
2735	8909	8957.6	0.99663	2641.38
2738	8916	8961.6	0.99644	2609.20
2817	9144	9060.7	1.01123	2747.89
2911	9070	9186.1	1.00187	2848.28

2935	9231	9211.4	1.02844	2938.70
2974	9236	9269.3	1.01235	2890.42
2987	9401	9285.4	1.01254	2848.27
3030	9177	9347.5	0.99457	2834.49
3031	9180	9348.2	0.99588	2839.84
3086	9317	9413.6	0.99046	3062.07
3181	9596	9540.0	1.00973	3022.99
3187	9549	9547.2	1.01179	3033.71
3217	9365	9592.5	0.98727	3037.55
3225	9666	9603.2	0.98821	3157.85
3238	9762	9614.2	1.00355	3213.79
3260	9477	9644.4	0.98727	3190.80
3274	9617	9655.6	1.01310	3265.14
3347	9775	9752.4	1.02526	3228.35
3361	9751	9781.7	1.00543	3208.43
3376	9803	9801.6	1.00430	3176.25
3381	9670	9807.6	0.99326	3183.91
3387	9609	9814.7	0.99532	3193.87
3400	9916	9828.9	1.00243	3322.60
3419	9866	9854.9	0.98615	3309.57
3463	9654	9901.4	1.00318	3416.85
3472	9697	9913.4	1.00281	3431.42
3481	9727	9931.5	0.99121	3396.93
3508	9861	9961.1	1.00711	3409.96
3508	9880	9961.1	1.00711	3409.96
3563	10117	10044.4	1.00468	3445.97
3629	10238	10127.7	1.00075	3578.54
3658	9876	10163.3	0.99345	3581.61
3736	10138	10273.5	0.98765	3510.34
3745	10162	10285.5	0.98578	3586.21
3772	10458	10315.1	1.01834	3608.43
3786	10341	10334.3	1.01591	3727.97
3930	10552	10524.0	0.98690	3734.10
3967	10384	10574.8	0.99944	3757.86
3988	10572	10603.2	0.99382	3858.24
4001	10572	10612.4	1.01853	3914.17
4041	10572	10660.0	1.01534	4030.65

(Page left blank)

Distribution

External Distribution

M. A. Adams
Jet Propulsion Laboratory
4800 Oak Grove Drive, MS 97
Pasadena, CA 91109

M. Aivazis
Center for Advanced Computing Research
California Institute of Technology
1200 E. California Blvd./MS 158-79
Pasadena, CA 91125

Charles E. Anderson
Southwest Research Institute
P. O. Drawer 28510
San Antonio, TX 78284-0510

Bilal Ayyub (2)
Department of Civil Engineering
University of Maryland
College Park, MD 20742-3021

Ivo Babuska
TICAM
Mail Code C0200
University of Texas at Austin
Austin, TX 78712-1085

Osman Balci
Department of Computer Science
Virginia Tech
Blacksburg, VA 24061

S. L. Barson
Boeing Company
Rocketdyne Propulsion & Power
MS IB-39
P. O. Box 7922
6633 Canoga Avenue
Canoga Park, CA 91309-7922

Steven Batill (2)
Dept. of Aerospace & Mechanical Engr.
University of Notre Dame
Notre Dame, IN 46556

S. Beissel
Alliant Techsystems, Inc.
600 Second St., NE
Hopkins, MN 55343

Ted Belytschko (2)
Department of Mechanical Engineering
Northwestern University
2145 Sheridan Road
Evanston, IL 60208

James Berger
Inst. of Statistics and Decision Science
Duke University
Box 90251
Durham, NC 27708-0251

(2)
Laboratory for Computational Physics and Fluid Dynamics
Naval Research Laboratory
Code 6400
4555 Overlook Ave, SW
Washington, DC 20375-5344

Pavel A. Bouzinov
ADINA R&D, Inc.
71 Elton Avenue
Watertown, MA 02472

John A. Cafeo
General Motors R&D Center
Mail Code 480-106-256
30500 Mound Road
Box 9055
Warren, MI 48090-9055

James C. Cavendish
General Motors R&D Center
Mail Code 480-106-359
30500 Mound Road
Box 9055
Warren, MI 48090-9055

Chun-Hung Chen (2)
Department of Systems Engineering & Operations Research
George Mason University
4400 University Drive, MS 4A6
Fairfax, VA 22030

Wei Chen
Dept. of Mechanical Engr. (M/C 251)
842 W. Taylor St.
University of Illinois at Chicago
Chicago, IL 60607-7022

Kyeongjae Cho (2)
Dept. of Mechanical Engineering
MC 4040
Stanford University
Stanford, CA 94305-4040

Thomas Chwastyk
U.S. Navel Research Lab.
Code 6304
4555 Overlook Ave., SW
Washington, DC 20375-5343

Harry Clark
Rocket Test Operations
AEDC
1103 Avenue B
Arnold AFB, TN 37389-1400

Hugh Coleman
Department of Mechanical &
Aero. Engineering
University of Alabama/Huntsville
Huntsville, AL 35899

Raymond Cosner (2)
Boeing-Phantom Works
MC S106-7126
P. O. Box 516
St. Louis, MO 63166-0516

Thomas A. Cruse
398 Shadow Place
Pagosa Springs, CO 81147-7610

Phillip Cuniff
U.S. Army Soldier Systems Center
Kansas Street
Natick, MA 01750-5019

Department of Energy (4)
Attn: Kevin Greenaugh, NA-115
B. Pate, DD-14
William Reed, DP-141
Jamileh Soudah, NA-114
1000 Independence Ave., SW
Washington, DC 20585

Prof. Urmila Diwekar (2)
University of Illinois at Chicago
Chemical Engineering Dept.
810 S. Clinton St.
209 CHB, M/C 110
Chicago, IL 60607

David Dolling
Department of Aerospace Engineering
& Engineering Mechanics
University of Texas at Austin
Austin, TX 78712-1085

Robert G. Easterling
51 Avenida Del Sol
Cedar Crest, NM 87008

Isaac Elishakoff
Dept. of Mechanical Engineering
Florida Atlantic University
777 Glades Road
Boca Raton, FL 33431-0991

Ashley Emery
Dept. of Mechanical Engineering
Box 352600
University of Washingtion
Seattle, WA 98195-2600

Scott Ferson
Applied Biomathematics
100 North Country Road
Setauket, New York 11733-1345

Joseph E. Flaherty (2)
Dept. of Computer Science
Rensselaer Polytechnic Institute
Troy, NY 12181

John Fortna
ANSYS, Inc.
275 Technology Drive
Canonsburg, PA 15317

Marc Garbey
Dept. of Computer Science
Univ. of Houston
501 Philipp G. Hoffman Hall
Houston, Texas 77204-3010

Roger Ghanem
Dept. of Civil Engineering
Johns Hopkins University
Baltimore, MD 21218

Mike Giltrud
Defense Threat Reduction Agency
DTRA/CPWS
6801 Telegraph Road
Alexandria, VA 22310-3398

James Glimm (2)
Dept. of Applied Math & Statistics
P138A
State University of New York
Stony Brook, NY 11794-3600

James Gran
SRI International
Poulter Laboratory AH253
333 Ravenswood Avenue
Menlo Park, CA 94025

Bernard Grossman (2)
Dept. of Aerospace &
Ocean Engineering
Mail Stop 0203
215 Randolph Hall
Blacksburg, VA 24061

Sami Habchi
CFD Research Corp.
Cummings Research Park
215 Wynn Drive
Huntsville, AL 35805

Raphael Haftka (2)
Dept. of Aerospace and Mechanical
Engineering and Engr. Science
P. O. Box 116250
University of Florida
Gainesville, FL 32611-6250

Achintya Haldar (2)
Dept. of Civil Engineering
& Engineering Mechanics
University of Arizona
Tucson, AZ 85721

Tim Hasselman
ACTA
2790 Skypark Dr., Suite 310
Torrance, CA 90505-5345

G. L. Havskjold
Boeing - Rocketdyne Propulsion & Power
MS GB-09
P. O. Box 7922
6633 Canoga Avenue
Canoga Park, CA 91309-7922

George Hazelrigg
Division of Design, Manufacturing
& Innovation
Room 508N
4201 Wilson Blvd.
Arlington, VA 22230

David Higdon
Inst. of Statistics and Decision Science
Duke University
Box 90251
Durham, NC 27708-0251

Richard Hills (25)
Mechanical Engineering Dept.
New Mexico State University
P. O. Box 30001/Dept. 3450
Las Cruces, NM 88003-8001

F. Owen Hoffman (2)
SENES
102 Donner Drive
Oak Ridge, TN 37830

Luc Huyse
Southwest Research Institute
6220 Culebra Road
P. O. Drawer 28510
San Antonio, TX 78284-0510

George Ivy
Northrop Grumman Information Technology
222 West Sixth St.
P.O. Box 471
San Pedro, CA 90733-0471

Ralph Jones (2)
Sverdrup Tech. Inc./AEDC Group
1099 Avenue C
Arnold AFB, TN 37389-9013

Leo Kadanoff (2)
Research Institutes Building
University of Chicago
5640 South Ellis Ave.
Chicago, IL 60637

George Karniadakis (2)
Division of Applied Mathematics
Brown University
192 George St., Box F
Providence, RI 02912

Alan Karr
Inst. of Statistics and Decision Science
Duke University
Box 90251
Durham, NC 27708-0251

J. J. Keremes
Boeing Company
Rocketdyne Propulsion & Power
MS AC-15
P. O. Box 7922
6633 Canoga Avenue
Canoga Park, CA 91309-7922

K. D. Kimsey
U.S. Army Research Laboratory
Weapons & Materials Research
Directorate
AMSRL-WM-TC 309 120A
Aberdeen Proving Gd, MD 21005-5066

B. A. Kovac
Boeing - Rocketdyne Propulsion & Power
MS AC-15
P. O. Box 7922
6633 Canoga Avenue
Canoga Park, CA 91309-7922

Chris Layne
AEDC
Mail Stop 6200
760 Fourth Street
Arnold AFB, TN 37389-6200

Ian Leslie (25)
Mechanical Engineering Dept.
New Mexico State University
P. O. Box 30001/Dept. 3450
Las Cruces, NM 88003-8001

W. K. Liu (2)
Northwestern University
Dept. of Mechanical Engineering
2145 Sheridan Road
Evanston, IL 60108-3111

Robert Lust
General Motors, R&D and Planning
MC 480-106-256
30500 Mound Road
Warren, MI 48090-9055

Sankaran Mahadevan (2)
Dept. of Civil &
Environmental Engineering
Vanderbilt University
Box 6077, Station B
Nashville, TN 37235

Hans Mair
Institute for Defense Analysis
Operational Evaluation Division
4850 Mark Center Drive
Alexandria VA 22311-1882

W. McDonald
NDM Solutions
1420 Aldenham Lane
Reston, VA 20190-3901

Gregory McRae (2)
Dept. of Chemical Engineering
Massachusetts Institute of Technology
Cambridge, MA 02139

Michael Mendenhall (2)
Nielsen Engineering & Research, Inc.
510 Clyde Ave.
Mountain View, CA 94043

Sue Minkoff (2)
Dept. of Mathematics and Statistics
University of Maryland
1000 Hilltop Circle
Baltimore, MD 21250

Max Morris (2)
Department of Statistics
Iowa State University
304A Snedecor-Hall
Ames, IW 50011-1210

R. Namburu
U.S. Army Research Laboratory
AMSRL-CI-H
Aberdeen Proving Gd, MD 21005-5067

NASA/Ames Research Center (2)
Attn: Unmeel Mehta, MS 229-3
David Thompson, MS 269-1
Moffett Field, CA 94035-1000

NASA/Glen Research Center (2)
Attn: John Slater, MS 86-7
Chris Steffen, MS 5-11
21000 Brookpark Road
Cleveland, OH 44135

NASA/Langley Research Center (7)
Attn: Dick DeLoach, MS 236
Michael Hemsch, MS 280
Tianshu Liu, MS 238
Jim Luckring, MS 280
Joe Morrison, MS 128
Ahmed Noor, MS 369
Sharon Padula, MS 159
Hampton, VA 23681-0001

C. Needham
Applied Research Associates, Inc.
4300 San Mateo Blvd., Suite A-220
Albuquerque, NM 87110

A. Needleman
Division of Engineering, Box D
Brown University
Providence, RI 02912

Robert Nelson
Dept. of Aerospace & Mechanical Engr.
University of Notre Dame
Notre Dame, IN 46556

Dick Neumann
8311 SE Millihanna Rd.
Olalla, WA 98359

Efstratios Nikolaidis (2)
MIME Dept.
4035 Nitschke Hall
University of Toledo
Toledo, OH 43606-3390

D. L. O'Connor
Boeing Company
Rocketdyne Propulsion & Power
MS AC-15
P. O. Box 7922
6633 Canoga Avenue
Canoga Park, CA 91309-7922

Tinsley Oden (2)
TICAM
Mail Code C0200
University of Texas at Austin
Austin, TX 78712-1085

Michael Ortiz (2)
Graduate Aeronautical Laboratories
California Institute of Technology
1200 E. California Blvd./MS 105-50
Pasadena, CA 91125

Dale Pace
Applied Physics Laboratory
Johns Hopkins University
111000 Johns Hopkins Road
Laurel, MD 20723-6099

Alex Pang
Computer Science Department
University of California
Santa Cruz, CA 95064

Allan Pifko
2 George Court
Melville, NY 11747

Cary Presser (2)
Process Measurements Div.
National Institute of Standards
and Technology
Bldg. 221, Room B312
Gaithersburg, MD 20899

Thomas A. Pucik
Pucik Consulting Services
13243 Warren Avenue
Los Angles, CA 90066-1750

P. Radovitzky
Graduate Aeronautical Laboratories
California Institute of Technology
1200 E. California Blvd./MS 105-50
Pasadena, CA 91125

W. Rafaniello
DOW Chemical Company
1776 Building
Midland, MI 48674

Chris Rahaim
1793 WestMeade Drive
Chesterfield, MO 63017

Pradeep Raj (2)
Computational Fluid Dynamics
Lockheed Martin Aeronautical Sys.
86 South Cobb Drive
Marietta, GA 30063-0685

J. N. Reddy
Dept. of Mechanical Engineering
Texas A&M University
ENPH Building, Room 210
College Station, TX 77843-3123

John Renaud (2)
Dept. of Aerospace & Mechanical Engr.
University of Notre Dame
Notre Dame, IN 46556

E. Repetto
Graduate Aeronautical Laboratories
California Institute of Technology
1200 E. California Blvd./MS 105-50
Pasadena, CA 91125

Patrick J. Roache
1108 Mesa Loop NW
Los Lunas, NM 87031

A. J. Rosakis
Graduate Aeronautical Laboratories
California Institute of Technology
1200 E. California Blvd./MS 105-50
Pasadena, CA 91125

Tim Ross (2)
Dept. of Civil Engineering
University of New Mexico
Albuquerque, NM 87131

J. Sacks
Inst. of Statistics and Decision Science
Duke University
Box 90251
Durham, NC 27708-0251

Sunil Saigal (2)
Carnegie Mellon University
Department of Civil and
Environmental Engineering
Pittsburgh, PA 15213

Larry Sanders
DTRA/ASC
8725 John J. Kingman Rd
MS 6201
Ft. Belvoir, VA 22060-6201

Len Schwer
Schwer Engineering & Consulting
6122 Aaron Court
Windsor, CA 95492

Paul Senseny
Factory Mutual Research Corporation
1151 Boston-Providence Turnpike
P.O. Box 9102
Norwood, MA 02062

E. Sevin
Logicon RDA, Inc.
1782 Kenton Circle
Lyndhurst, OH 44124

Mark Shephard (2)
Rensselaer Polytechnic Institute
Scientific Computation Research Center
Troy, NY 12180-3950

Tom I-P. Shih
Dept. of Mechanical Engineering
2452 Engineering Building
East Lansing, MI 48824-1226

T. P. Shivananda
Bldg. SB2/Rm. 1011
TRW/Ballistic Missiles Division
P. O. Box 1310
San Bernardino, CA 92402-1310

Y.-C. Shu
Graduate Aeronautical Laboratories
California Institute of Technology
1200 E. California Blvd./MS 105-50
Pasadena, CA 91125

Don Simons
Northrop Grumman Information Tech.
222 W. Sixth St.
P.O. Box 471
San Pedro, CA 90733-0471

Munir M. Sindir
Boeing - Rocketdyne Propulsion & Power
MS GB-11
P. O. Box 7922
6633 Canoga Avenue
Canoga Park, CA 91309-7922

Ashok Singhal (2)
CFD Research Corp.
Cummings Research Park
215 Wynn Drive
Huntsville, AL 35805

R. Singleton
Engineering Sciences Directorate
Army Research Office
4300 S. Miami Blvd.
P.O. Box 1221
Research Triangle Park, NC 27709-2211

W. E. Snowden
DARPA
7120 Laketree Drive
Fairfax Station, VA 22039

Bill Spencer (2)
Dept. of Civil Engineering
and Geological Sciences
University of Notre Dame
Notre Dame, IN 46556-0767

Fred Stern
Professor Mechanical Engineering
Iowa Institute of Hydraulic Research
The University of Iowa
Iowa City Iowa 52242

D. E. Stevenson (2)
Computer Science Department
Clemson University
442 Edwards Hall, Box 341906
Clemson, SC 29631-1906

Tim Swafford
Sverdrup Tech. Inc./AEDC Group
1099 Avenue C
Arnold AFB, TN 37389-9013

Kenneth Tatum
Sverdrup Tech. Inc./AEDC Group
740 Fourth Ave.
Arnold AFB, TN 37389-6001

Ben Thacker
Southwest Research Institute
6220 Culebra Road
P. O. Drawer 28510
San Antonio, TX 78284-0510

Fulvio Tonon (2)
Geology and Geophysics Dept.
East Room 719
University of Utah
135 South 1460
Salt Lake City, UT 84112

Robert W. Walters (2)
Aerospace and Ocean Engineering
Virginia Tech
215 Randolph Hall, MS 203
Blacksburg, VA 24061-0203

Leonard Wesley
Intellex Inc.
5932 Killarney Circle
San Jose, CA 95138

Justin Y-T Wu
8540 Colonnade Center Drive, Ste 301
Raleigh, NC 27615

Ren-Jye Yang
Ford Research Laboratory
MD2115-SRL
P.O.Box 2053
Dearborn, MI 4812

Simone Youngblood (2)
DOD/DMSO
Technical Director for VV&A
1901 N. Beauregard St., Suite 504
Alexandria, VA 22311

M. A. Zikry
North Carolina State University
Mechanical & Aerospace Engineering
2412 Broughton Hall, Box 7910
Raleigh, NC 27695

Foreign Distribution

Yakov Ben-Haim (2)
Department of Mechanical Engineering
Technion-Israel Institute of Technology
Haifa 32000
ISRAEL

Gert de Cooman (2)
Universiteit Gent
Onderzoeksgroep, SYSTeMS
Technologiepark - Zwijnaarde 9
9052 Zwijnaarde
BELGIUM

Graham de Vahl Davis
CFD Research Laboratory
University of NSW
Sydney, NSW 2052
AUSTRALIA

Luis Eca (2)
Instituto Superior Tecnico
Department of Mechanical Engineering
Av. Rovisco Pais
1096 Lisboa CODEX
PORTUGAL

Charles Hirsch (2)
Department of Fluid Mechanics
Vrije Universiteit Brussel
Pleinlaan, 2
B-1050 Brussels
BELGIUM

Igor Kozin (2)
Systems Analysis Department
Riso National Laboratory
P. O. Box 49
DK-4000 Roskilde
DENMARK

K. Papoulia
Inst. Eng. Seismology & Earthquake Engineering
P.O. Box 53, Finikas GR-55105
Thessaloniki
GREECE

Dominique Pelletier
Genie Mecanique
Ecole Polytechnique de Montreal
C.P. 6079, Succursale Centre-ville
Montreal, H3C 3A7
CANADA

Lev Utkin
Institute of Statistics
Munich University
Ludwigstr. 33
80539, Munich
GERMANY

Malcolm Wallace
Computational Dynamics Ltd.
200 Shepherds Bush Road
London W6 7NY
UNITED KINGDOM

Peter Walley
6 Jewel Close
Port Douglas
Queensland 4871
AUSTRALIA

Department of Energy Laboratories

Los Alamos National Laboratory (53)
Mail Station 5000
P.O. Box 1663
Los Alamos, NM 87545
Attn: Peter Adams, MS B220
Mark C. Anderson, MS D411
Robert Benjamin, MS P940
Jane M. Booker, MS P946
Terrence Bott, MS K557
Jerry S. Brock, MS D413
D. Cagliostro, MS F645
Katherine Campbell, MS F600
David L. Crane, MS P946
John F. Davis, MS B295
Helen S. Deaven, MS B295
Barbara DeVolder, MS B259
Scott Doebling, MS P946
S. Eisenhawer, MS K557
Dawn Flicker, MS F664
George T. Gray, MS G755
Ken Hanson, MS B250
Alexandra Heath, MS F663
R. Henninger, MS D413
Brad Holian, MS B268
Kathleen Holian, MS B295
Darryl Holm, MS B284
James Hyman, MS B284
Valen Johnson, MS F600
Cliff Joslyn, MS B265
James Kamm, MS D413
S. Keller-McNulty, MS F600
Joseph Kindel, MS B259
Ken Koch, MS F652
Douglas Kothe, MS B250
Jeanette Lagrange, MS D445
Len Margolin, MS D413
Harry Martz, MS F600
Mike McKay, MS F600
Kelly McLenithan, MS F664
Mark P. Miller, MS P946
John D. Morrison, MS F602
Karen I. Pao, MS B256
James Peery, MS F652
M. Peterson-Schnell, MS B295
Douglas Post, MS F661 X-DO
William Rider, MS D413
Tom Seed, MS F663
Kari Sentz, MS B265
David Sharp, MS B213
Richard N. Silver, MS D429
Ronald E. Smith, MS J576
Christine Treml, MS H851
David Tubbs, MS B220
Daniel Weeks, MS B295
Morgan White, MS F663
Alyson G. Wilson, MS F600

Lawrence Livermore National Laboratory (21)
7000 East Ave.
P.O. Box 808
Livermore, CA 94550
Attn: Thomas F. Adams, MS L-095
Steven Ashby, MS L-561
John Bolstad, MS L-023
Peter N. Brown, MS L-561
T. Scott Carman, MS L-031
R. Christensen, MS L-160
Evi Dube, MS L-095
Henry Hsieh, MS L-229
Richard Klein, MS L-023
Roger Logan, MS L-125
C. F. McMillan, MS L-098
C. Mailhiot, MS L-055
J. F. McEnerney, MS L-023
M. J. Murphy, MS L-282
Daniel Nikkel, MS L-342
Cynthia Nitta, MS L-096
Peter Raboin, MS L-125
Kambiz Salari, MS L-228
Peter Terrill, MS L-125
Charles Tong, MS L-560
Carol Woodward, MS L-561

Argonne National Laboratory
Attn: Paul Hovland
MCS Division
Bldg. 221, Rm. C-236
9700 S. Cass Ave.
Argonne, IL 60439

SANDIA INTERNAL

1	MS 1152	1642	M. L. Kiefer
1	MS 1186	1674	R. J. Lawrence
1	MS 0525	1734	P. V. Plunkett
1	MS 0525	1734	R. B. Heath
1	MS 0525	1734	S. D. Wix
1	MS 0429	2100	J. S. Rottler
1	MS 0429	2100	R. C. Hartwig
1	MS 0447	2111	P. Davis
1	MS 0447	2111	P. D. Hoover

1	MS 0479	2113	J. O. Harrison
1	MS 0487	2115	P. A. Sena
1	MS 0453	2130	H. J. Abeyta
1	MS 0482	2131	K. D. Meeks
1	MS 0482	2131	R. S. Baty
1	MS 0481	2132	M. A. Rosenthal
1	MS 0427	2134	R. A. Paulsen
1	MS 0509	2300	M. W. Callahan
1	MS 0645	2912	D. R. Olson
1	MS 0634	2951	K. V. Chavez
1	MS 0769	5800	D. S. Miyoshi
1	MS 0735	6115	S. C. James
1	MS 0751	6117	L. S. Costin
1	MS 0708	6214	P. S. Veers
1	MS 0490	6252	J. A. Cooper
1	MS 0736	6400	T. E. Blejwas
1	MS 0744	6400	D. A. Powers
1	MS 0747	6410	A. L. Camp
1	MS 0747	6410	G. D. Wyss
1	MS 0748	6413	D. G. Robinson
1	MS 0748	6413	R. D. Waters
1	MS 0576	6536	L. M. Claussen
1	MS 1137	6536	G. K. Froehlich
1	MS 1137	6536	A. L. Hodges
1	MS 1138	6536	M. T. McCornack
1	MS 1137	6536	S. V. Romero
1	MS 1137	6544	S. M. DeLand
1	MS 1137	6545	L. J. Lehoucq
1	MS 1137	6545	G. D. Valdez
1	MS 0720	6804	P. G. Kaplan
1	MS 1395	6820	M. J. Chavez
1	MS 1395	6821	M. K. Knowles
1	MS 1395	6821	J. W. Garner
1	MS 1395	6821	E. R. Giambalvo
1	MS 1395	6821	J. S. Stein
1	MS 0779	6840	M. G. Marietta
1	MS 0779	6840	P. Vaughn
1	MS 0779	6849	J. C. Helton
1	MS 0779	6849	L. C. Sanchez
1	MS 0778	6851	G. E. Barr
1	MS 0778	6851	R. J. MacKinnon
1	MS 0778	6851	P. N. Swift
1	MS 0776	6852	B. W. Arnold
1	MS 0776	6852	T. Hadgu
1	MS 0776	6852	R. P. Rechard
1	MS 9001	8000	J. L. Handrock
1	MS 9007	8200	D. R. Henson
1	MS 9202	8205	R. M. Zurn
1	MS 9005	8240	E. T. Cull, Jr.
1	MS 9051	8351	C. A. Kennedy
1	MS 9405	8700	R. H. Stulen
1	MS 9404	8725	J. R. Garcia
1	MS 9404	8725	W. A. Kawahara
1	MS 9161	8726	E. P. Chen
1	MS 9405	8726	R. E. Jones
1	MS 9161	8726	P. A. Klein
1	MS 9405	8726	R. A. Regueiro
1	MS 9042	8727	J. J. Dike
1	MS 9042	8727	A. R. Ortega
1	MS 9042	8728	C. D. Moen
1	MS 9003	8900	K. E. Washington
1	MS 9003	8940	C. M. Hartwig
1	MS 9217	8962	P. D. Hough
1	MS 9217	8962	K. R. Long
1	MS 9217	8962	M. L. Martinez-Canales
1	MS 9217	8962	J. C. Meza
1	MS 9012	8964	P. E. Nielan
1	MS 0841	9100	T. C. Bickel
1	MS 0841	9100	C. W. Peterson
1	MS 0826	9100	D. K. Gartling
1	MS 0824	9110	A. C. Ratzel
1	MS 0834	9112	M. R. Prairie
1	MS 0834	9112	S. J. Beresh
1	MS 0835	9113	S. N. Kempka
1	MS 0834	9114	J. E. Johannes
1	MS 0834	9114	K. S. Chen
1	MS 0834	9114	R. R. Rao
1	MS 0834	9114	P. R. Schunk
1	MS 0825	9115	B. Hassan
1	MS 0825	9115	F. G. Blottner
1	MS 0825	9115	D. W. Kuntz
1	MS 0825	9115	M. A. McWherter Payne
1	MS 0825	9115	J. L. Payne
1	MS 0825	9115	D. L. Potter
1	MS 0825	9115	C. J. Roy
1	MS 0825	9115	W. P. Wolfe
1	MS 0836	9116	E. S. Hertel
1	MS 0836	9116	D. Dobranich
1	MS 0836	9116	R. E. Hogan
1	MS 0836	9116	C. Romero
1	MS 0836	9117	R. O. Griffith
1	MS 0836	9117	R. J. Buss
1	MS 0847	9120	H. S. Morgan
1	MS 0555	9122	M. S. Garrett
1	MS 0893	9123	R. M. Brannon
1	MS 0847	9124	J. M. Redmond
1	MS 0557	9124	T. G. Carne
1	MS 0847	9124	R. V. Field
1	MS 0557	9124	T. Simmermacher
1	MS 0553	9124	D. O. Smallwood
1	MS 0847	9124	S. F. Wojtkiewicz
1	MS 0557	9125	T. J. Baca

1	MS 0557	9125	C. C. O'Gorman
1	MS 0847	9126	R. A. May
1	MS 0847	9126	S. N. Burchett
1	MS 0847	9126	T. D. Hinnerichs
1	MS 0847	9126	K. E. Metzinger
1	MS 0847	9127	J. Jung
1	MS 0824	9130	J. L. Moya
1	MS 1135	9132	L. A. Gritzo
1	MS 1135	9132	J. T. Nakos
1	MS 1135	9132	S. R. Tieszen
3	MS 0828	9133	M. Pilch
1	MS 0828	9133	A. R. Black
1	MS 0828	9133	B. F. Blackwell
1	MS 0828	9133	K. J. Dowding
5	MS 0828	9133	W. L. Oberkampf
1	MS 0557	9133	T. L. Paez
1	MS 0847	9133	J. R. Red-Horse
1	MS 0828	9133	V. J. Romero
1	MS 0828	9133	M. P. Sherman
1	MS 0557	9133	A. Urbina
1	MS 0847	9133	W. R. Witkowski
1	MS 1135	9134	S. Heffelfinger
1	MS 0847	9134	S. W. Attaway
1	MS 0835	9140	J. M. McGlaun
1	MS 0835	9141	E. A. Boucheron
1	MS 0847	9142	K. F. Alvin
1	MS 0847	9142	M. L. Blanford
1	MS 0847	9142	M. W. Heinstein
1	MS 0847	9142	S. W. Key
1	MS 0847	9142	G. M. Reese
1	MS 0826	9143	J. D. Zepper
1	MS 0827	9143	K. M. Aragon
1	MS 0827	9143	H. C. Edwards
1	MS 0847	9143	G. D. Sjaardema
1	MS 0826	9143	J. R. Stewart
1	MS 0321	9200	W. J. Camp
1	MS 0318	9200	G. S. Davidson
1	MS 0847	9211	S. A. Mitchell
1	MS 0847	9211	M. S. Eldred
1	MS 0847	9211	A. A. Giunta
1	MS 1110	9211	A. Johnson
5	MS 0819	9211	T. G. Trucano
1	MS 0847	9211	B. G. vanBloemen Waanders
1	MS 0316	9212	S. J. Plimpton
1	MS 1110	9214	D. E. Womble
1	MS 1110	9214	J. DeLaurentis
1	MS 1110	9214	R. B. Lehoucq
1	MS 1111	9215	B. A.Hendrickson
1	MS 1110	9215	R. Carr
1	MS 1110	9215	S. Y. Chakerian
1	MS 1110	9215	W. E. Hart
1	MS 1110	9215	V. J. Leung
1	MS 1110	9215	C. A. Phillips
1	MS 1109	9216	R. J. Pryor
1	MS 0310	9220	R. W. Leland
1	MS 0310	9220	J. A. Ang
1	MS 1110	9223	N. D. Pundit
1	MS 1110	9224	D. W. Doerfler
1	MS 0847	9226	P. Knupp
1	MS 0822	9227	P. D. Heermann
1	MS 0822	9227	C. F. Diegert
1	MS 0318	9230	P. Yarrington
1	MS 0819	9231	R. M. Summers
1	MS 0819	9231	K H. Brown
1	MS 0819	9231	K. G. Budge
1	MS 0819	9231	S. P. Burns
1	MS 0819	9231	D. E. Carroll
1	MS 0819	9231	M. A. Christon
1	MS 0819	9231	R. R. Drake
1	MS 0819	9231	A. C. Robinson
1	MS 0819	9231	M. K. Wong
1	MS 0820	9232	P. F. Chavez
1	MS 0820	9232	M. E. Kipp
1	MS 0820	9232	S. A. Silling
1	MS 0820	9232	R. M. Summers
1	MS 0820	9232	P. A. Taylor
1	MS 0820	9232	J. R. Weatherby
1	MS 0316	9233	S. S. Dosanjh
1	MS 0316	9233	D. R. Gardner
1	MS 0316	9233	S. A. Hutchinson
1	MS 1111	9233	A. G. Salinger
1	MS 1111	9233	J. N. Shadid
1	MS 0316	9235	J. B. Aidun
1	MS 0316	9235	H. P. Hjalmarson
1	MS 0660	9514	M. A. Ellis
1	MS 0660	9519	D. S. Eaton
1	MS 0421	9800	W. Hermina
1	MS 0139	9900	M. O. Vahle
1	MS 0139	9904	R. K. Thomas
1	MS 0139	9905	S. E. Lott
1	MS 0428	12300	D. D. Carlson
1	MS 0428	12301	V. J. Johnson
1	MS 0638	12316	M. A. Blackledge
1	MS 0638	12316	D. L. Knirk
1	MS 0638	12316	D. E. Peercy
1	MS 0829	12323	W. C. Moffatt
1	MS 0829	12323	J. M. Sjulin
1	MS 0829	12323	B. M. Rutherford
1	MS 0829	12323	F. W. Spencer
1	MS 0405	12333	T. R. Jones
1	MS 0405	12333	M. P. Bohn
1	MS 0405	12333	S. E. Camp
1	MS 0434	12334	R. J. Breeding

1	MS 0830	12335	K. V. Diegert
1	MS 1030	12870	J. G. Miller
1	MS 1170	15310	R. D. Skocypec
1	MS 1176	15312	R. M. Cranwell
1	MS 1176	15312	D. J. Anderson
1	MS 1176	15312	J. E. Campbell
1	MS 1176	15312	L. P. Swiler
1	MS 1179	15340	J. R. Lee
1	MS 1179	15341	L. Lorence
1	MS 1164	15400	J. L. McDowell
1	MS 1174	15414	W. H. Rutledge
1	MS 9018	8945-1	Central Technical Files
2	MS 0899	9616	Technical Library
1	MS 0612	9612	Review & Approval Desk For DOE/OSTI